1996

Modeling Diseased Oyster Populations. II. Triggering Mechanisms for Perkinsus marinus Epizootics

Eric N. Powell

John M. Klinck
Old Dominion University, jklinck@odu.edu

Eileen E. Hofmann
Old Dominion University, ehofmann@odu.edu

Original Publication Citation

Powell, E. N., Klinck, J. M., & Hofmann, E. E. (1996). Modeling diseased oyster populations. II. Triggering mechanisms for *Perkinsus marinus* epizootics. *Journal of Shellfish Research, 15*(1), 141-165.

Journal of Shellfish Research, Vol. 15, No. 1, 141–165, 1996.

MODELING DISEASED OYSTER POPULATIONS. II. TRIGGERING MECHANISMS FOR *PERKINSUS MARINUS* EPIZOOTICS

ERIC N. POWELL,[1,3] JOHN M. KLINCK,[2] AND EILEEN E. HOFMANN[2]

[1]*Department of Oceanography*
Texas A&M University
College Station, Texas 77843
[2]*Center for Coastal Physical Oceanography*
Crittenton Hall
Old Dominion University
Norfolk, Virginia 23529

ABSTRACT Densities of *Crassostrea virginica* remain high enough to support substantial fisheries throughout the Gulf of Mexico despite high mortality rates produced by the endoparasite *Perkinsus marinus*. The infrequency of epizootics in these populations suggests that controls exist on the disease intensification process. The progression of epizootics in oyster populations, the factors that trigger epizootics, and the factors that terminate epizootics once started were investigated with a coupled oyster population–*P. marinus* model.

The time development of a simulated epizootic was triggered by environmental conditions that occurred and disappeared as much as 18 months prior to the onset of mortality in the oyster population. Initiation of epizootic conditions was detected as an increase in infection intensity in the submarket-size adult and juvenile portions of the oyster population. Infection intensity of the market-size adults is maintained at a relatively stable level by the death of heavily infected individuals and the slow rate of *P. marinus* division at high infection intensities. Once started, most of the simulated epizootics resulted in population extinction in 2 to 4 years. Stopping an epizootic required reducing the infection intensity in the submarket-size adults and juveniles. The infection intensity of market-size adults does not need to be reduced to stop an epizootic nor must it be raised to start one.

The simulated oyster populations show that a reduction in ingestion rate (by reduced food supply or increased turbidity) can trigger an epizootic, especially if the reduction occurs during the summer. Increasing food supply or decreasing turbidity in the following year does not necessarily prevent the occurrence of an epizootic. Rather, the onset of the event is simply delayed. Additional simulations show that the relative combination of variations in salinity and temperature is important in determining the occurrence of an epizootic. A dry (high-salinity) summer followed by a warm winter produces conditions that favor the development of an epizootic. Conversely, a warm dry year followed by a cool wet year fails to produce an epizootic. Simulations that consider variations in the biological characteristics of oyster populations, such as changes in recruitment rate or disease resistance, show that these are important in regulating the occurrence of an epizootic as well as in terminating the event. In particular, increased recruitment rate dilutes the infected population sufficiently to terminate an epizootic.

One primary conclusion that can be obtained from these simulations is that epizootics of *P. marinus* in oyster populations are difficult to generate simply with changes in either temperature or salinity. Rather, the epizootics are triggered by some other factor, such as reduced food supply or reduced recruitment rate, that occurs prior to or coincident with high salinity or temperature conditions.

KEY WORDS: *Perkinsus marinus* disease, disease model, oyster disease, eastern oysters, *Crassostrea virginica*

INTRODUCTION

Throughout the southern extent of their habitat range, populations of the eastern oyster, *Crassostrea virginica*, are impacted greatly by the disease-producing endoparasite *Perkinsus marinus* (Quick and Mackin 1971, Wilson et al. 1990, Lewis et al. 1992). In the Gulf of Mexico, the market-size component of oyster populations generally suffers about 50% yearly mortality due to *P. marinus* (Mackin 1961, 1962, Hofstetter 1977). Only one Gulf of Mexico oyster population is known to be free of infection from *P. marinus* (Powell et al. 1992a). Typically, prevalence of this organism exceeds 60% in nearly all populations (Craig et al. 1989, Wilson et al. 1990). Similar conditions exist in oyster populations along the southeastern coast of the United States (Crosby and Roberts 1990, Hofmann et al. 1995). However, despite high disease prevalence and high mortality rates, *C. virginica* generally maintains healthy population densities, which support substantial fisheries throughout much of the range of this animal (Hofstetter 1990, NOAA 1991, Powell et al. 1995b).

Nevertheless, epizootics produced by *P. marinus* do occasionally occur throughout the range of *P. marinus*, although those occurring in the mid-Atlantic region have been more noteworthy in their areal extent and effect on the fishery (Mann et al. 1991, Sindermann 1993). Epizootics of most animal species follow a series of characteristic stages (Gill 1928), which are shown schematically in Figure 1. Most are triggered during a preepizootic phase when the host population appears to be at its healthiest (Gill 1928). The triggering mechanism does not need to remain after the initiation of epizootic conditions. In fact, most mortality usually occurs a significant time after the conditions triggering the epizootic have disappeared. Recovery occurs during the postepizootic phase and the population remains in quasiequilibrium with the disease during a potentially extended interepizootic phase during which time the host population abundance normally increases (e.g., Ross 1982, McCallum and Singleton 1989).

Most models of the factors that trigger and/or control epizootics stress the role of transmission rates and the relative proportion of the population that is susceptible to the disease (Ackerman et al.

[3]Present address: Haskin Shellfish Research Laboratory, Rutgers University, Port Norris, NJ 08349.

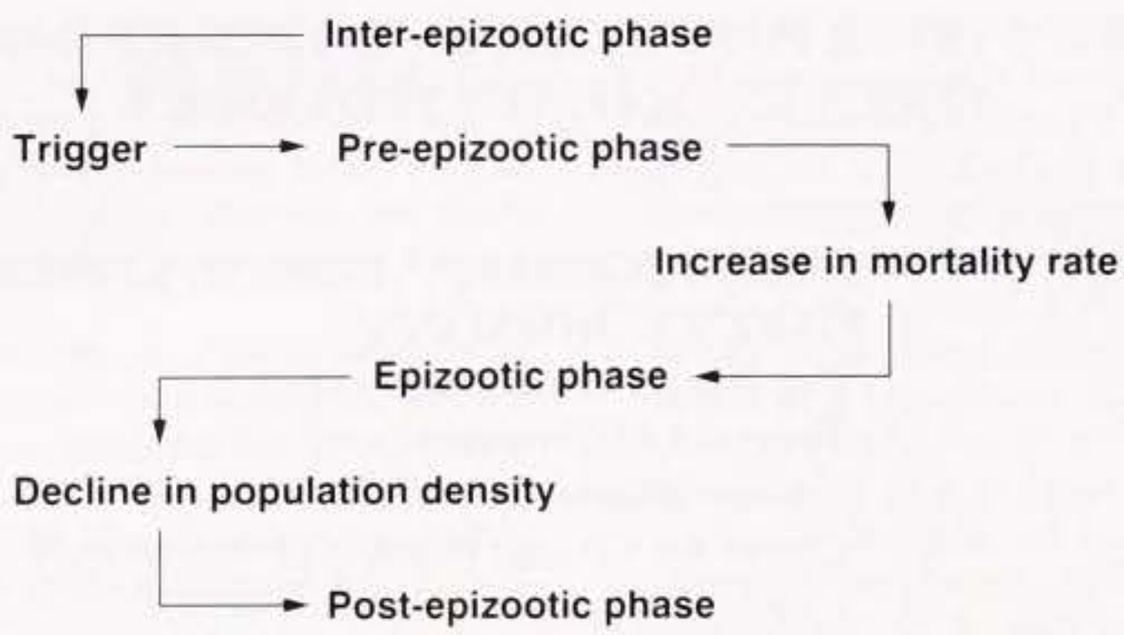

Figure 1. Schematic of the stages that are associated with an epizootic.

1984, Mollison 1987, Kermack and McKendrick 1991a,b, Anderson 1991, Dwyer and Elkinton 1993). Typical triggers for epizootics involve factors that vary contact rates, prevalences, and the behavior of susceptible individuals. *P. marinus*, however, presents a relatively unusual case. Disease prevalence in most oyster populations during the interepizootic phase is high. Thus, variations in disease transmission rates are of lesser consequence. Most oyster populations retain a balance between disease intensification and oyster population expansion that favors the oyster population and the breakdown of this balance initiates an epizootic.

The relative infrequency of epizootics in oyster populations routinely existing with disease prevalences of 80% or more suggests that controls exist that operate on the disease intensification process but not on the transmission process. One such control is suggested by experimental studies that have shown that the doubling time of *P. marinus* is reduced at high infection intensities. This permits oysters to survive at infection intensities that are only a few doublings from lethal levels (Saunders et al. 1993). Also, high fecundity rates, particularly in the spring and early summer when infection intensities are low in the younger, less heavily infected adults (Choi et al. 1994), result in the introduction of uninfected individuals into the population, which dilutes the mean disease intensity.

Under normal conditions, mortality from *P. marinus* infection does not exceed the rate of oyster population expansion and the oyster population remains healthy even though suffering substantial mortality from the disease. The infrequency of epizootics in *P. marinus*–infected oyster populations suggests that triggering mechanisms must exist that permit the rate of disease intensification to override the rates of oyster population expansion for a time. Once this threshold is crossed, the disease process is sufficient to reduce population growth and fecundity, and subsequently recruitment, so that the population slips inexorably toward extinction. Epizootics are generally associated with high salinities; however, other triggering mechanisms may exist. Generally, these should be factors that reduce oyster growth rate or fecundity or adversely affect the ability of the oyster to fight the disease.

Once started, an epizootic may prove to be difficult to stop because most progress until host mortality reduces the population density to a level that can no longer sustain the disease. This critical population density is normally determined by the transmission rate (Bartlett 1960, Black 1966, Mollison 1987, Anderson 1991). When transmission rate is high, as it is for *P. marinus*, this critical population density is usually very low. Thus, local extinction of the host population is a likely outcome of a *P. marinus* epizootic (e.g., Plowright 1982, Mollison 1987).

The objectives of this paper are to investigate the progression of *P. marinus* epizootics in oyster populations, the factors that trigger these epizootics, and the factors that can terminate an epizootic once it is started. These objectives are addressed using a coupled oyster population–*P. marinus* model. A series of simulations are presented that are designed to investigate the role of environmental factors, competition from other filter feeders, population recruitment rates, and disease resistance in triggering epizootics of *P. marinus*. Additional simulations consider the environmental and biological factors that can stop an epizootic. The simulations primarily use idealized time series of environmental variables designed to illustrate specific points. However, measured environmental conditions from Galveston Bay, Texas, a mid-latitude bay where *P. marinus* infects almost 100% of the oyster population, are used where appropriate.

THE OYSTER POPULATION—*PERKINSUS MARINUS* MODEL

General Characteristics

The host-parasite model (Fig. 2) consists of separate models for the dynamics of the postsettlement oyster population and the growth of *P. marinus*. The two models are coupled by relationships that describe the removal of oyster energy by the parasite to support its metabolic requirements and relationships that relate the rates of parasite division and mortality to host mortality. The oyster population model, described in detail by Hofmann et al. (1992, 1995) and Powell et al. (1992b, 1994, 1995a), consists of a size-structured model that considers the processes regulating the growth and death of the oyster from newly settled juveniles to adults. The description of this model will focus on only the modifications made to allow connection between the parasite and host components. The *P. marinus* model includes metabolic growth and loss processes as well as a component that describes the transmission of the disease. The parasite model, which uses infection level as the state variable, is described in detail following a brief review of the oyster population model.

Governing Equation

The time change in oyster standing stock ($O_{j,k}$) in each oyster size class (j) and *P. marinus* infection level (k) is the result of changes in net production ($NP_{j,k}$), which is the sum of the production of somatic ($Pg_{j,k}$) and reproductive ($Pr_{j,k}$) tissue, and the addition of individuals from the previous size class or loss to the next largest size class by growth. Oyster net production is assumed to be the difference between assimilation ($A_{j,k}$) and respiration ($R_{j,k}$), as discussed by White et al. (1988), and losses to *P. marinus* ($E_{j,k}$) and is expressed as:

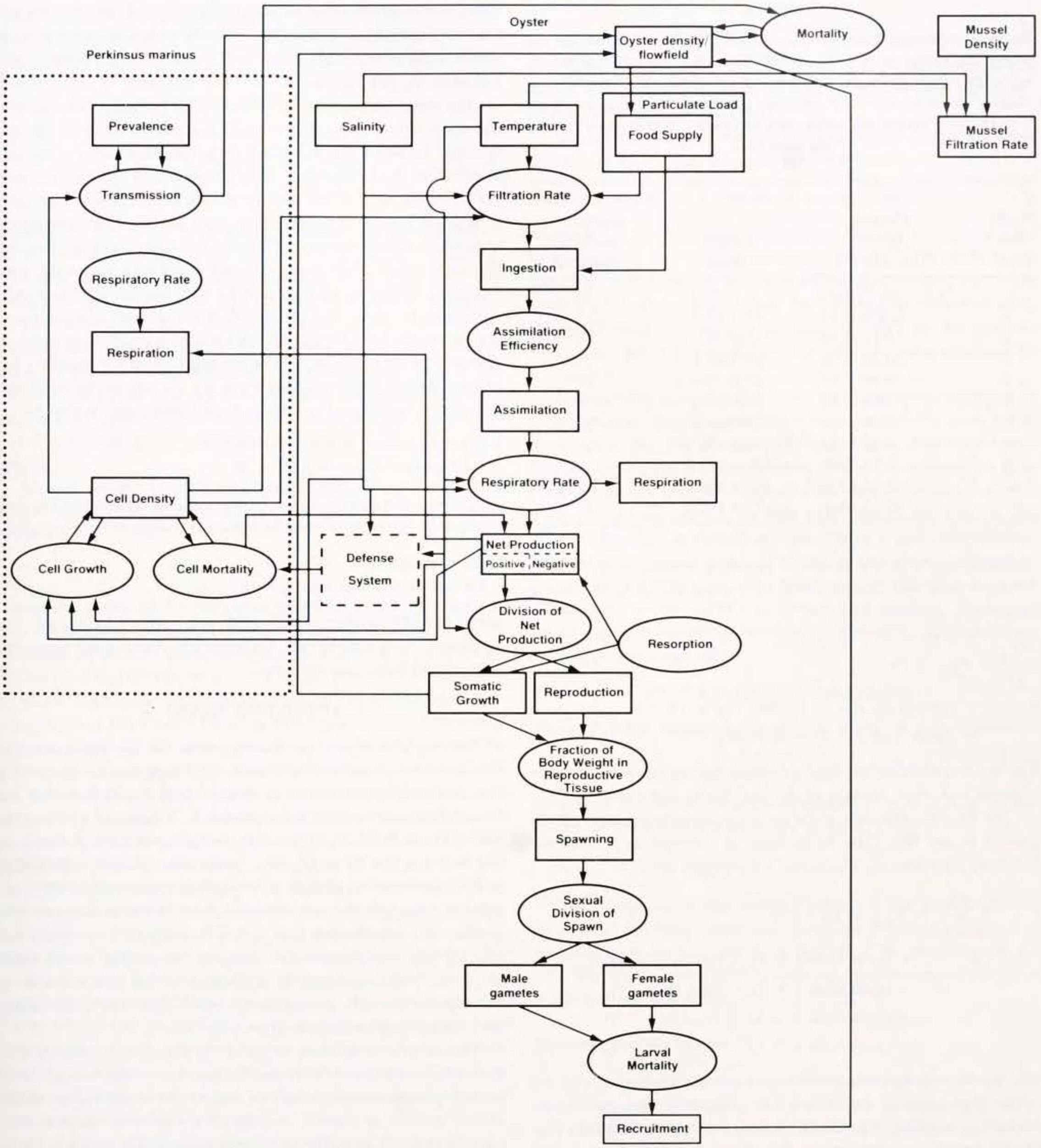

Figure 2. Schematic of the coupled oyster population–*P. marinus* population dynamics model.

$$NP_{j,k} = Pg_{j,k} + Pr_{j,k} = A_{j,k} - R_{j,k} - E_{j,k}. \quad (1)$$

The governing equation for the oyster population is then:

$$\frac{dO_{j,k}}{dt} = Pg_{j,k} + Pr_{j,k} + (\text{gain from } j-1) - (\text{loss to } j+1) \quad (2)$$

where $j = 1,11$, which represents the size class partitioning of the oyster life history. The last two terms on the right side represent gains and losses in a particular size class by individuals gaining biomass and moving to the next higher size class. Size is defined in terms of biomass (g AFDW) rather than length (Table 1). Reproductive tissue formation is zero for the first three size classes, which represent juveniles.

During suboptimal conditions, oysters can resorb gonadal or somatic tissue and hence lose biomass ($NP_{j,k} < 0$) and transfer into the next lower size class. Thus, biomass can change during periods of negative scope for growth, which is the basis for the use of

TABLE 1.

Biomass and length dimensions and lethal *P. marinus* density for the oyster size classes used in the model. Biomass is converted to length using the relationship given in White et al. (1988). Mortality level is defined as the number of *P. marinus* population doublings required to reach or exceed the lethal parasite density as calculated from equation (24).

Model Size Class	Biomass (g ash free dry wt)	Length (mm)	Mortality Level (population doublings required)
1	1.3×10^{-7}–0.028	0.3–25.0	21
2	0.028–0.10	25.0–35.0	23
3	0.10–0.39	35.0–50.0	24
4	0.39–0.98	50.0–63.5	25
5	0.98–1.44	63.5–70.0	26
6	1.44–1.94	70.0–76.0	26
7	1.94–3.53	76.0–88.9	26
8	3.53–5.52	88.9–100.0	27
9	5.52–7.95	100.0–110.0	27
10	7.95–12.93	110.0–125.0	27
11	12.93–25.91	125.0–150.0	27

condition index as a measure of health in oysters (e.g., Newell 1985, Wright and Hetzel 1985). To allow for this, the above equation is modified as:

$$\frac{dO_{j,k}}{dt} = Pg_{j,k} + Pr_{j,k} + (\text{gain from } j-1) - (\text{loss to } j+1) + (\text{gain from } j+1) - (\text{loss to } j-1) \quad (3)$$

The last two terms on the right side represent the individuals losing biomass and, thus, moving to the next lower size class.

The final modification to the oyster-governing equation allows oysters in any size class to increase or decrease in *P. marinus* infection intensity:

$$\frac{dO_{j,k}}{dt} = Pg_{j,k} + Pr_{j,k} + (\text{gain from } j-1) - (\text{loss to } j+1) + (\text{gain from } j+1) - (\text{loss to } j-1) + (\text{gain from } k-1) - (\text{loss to } k+1) + (\text{gain from } k+1) - (\text{loss to } k-1). \quad (4)$$

The last four terms represent changes in infection intensity of the oyster population as the *P. marinus* population increases or decreases in number. The model includes 28 predefined infection levels. Level 1 consists of uninfected oysters. The remaining 27 levels represent degrees of infection that correspond to the number of doublings of the *P. marinus* population beginning with one cell in level 2.

Three aspects of the model given by the above equation deserve note. First, settlement of juvenile oysters (as spat) occurs exclusively in the first size class ($j = 1$) and first infection level ($k = 1$). These newly recruited individuals are uninfected by *P. marinus*. Second, movement of oysters from the uninfected to the newly infected stage occurs by the acquisition of one infective cell (infection level 2) and occurs only in the positive direction, a gain of infection. Infections, once acquired by oysters, are never lost (Andrews 1988). Finally, once the oysters have reached the infection level defined as lethal (Table 1), they are classified as dead and both the *P. marinus* and the oyster biomasses are permanently lost from the population.

The gain, loss, or transfer of energy (or biomass) between size classes or across infection levels is expressed in terms of specific rates (d^{-1}), which are multiplied by the caloric quantity in the size or infection class. Transfers of oysters between size classes were scaled by the ratio of the average weight of the current size class (in g dry wt) to that of the size class from which energy was gained or to which energy was lost. This scaling, made necessary because the oyster size classes were unevenly distributed across the size-frequency spectrum, ensured that the total number of oyster individuals in the model was conserved, in the absence of recruitment and mortality, even though all calculations were done in terms of calories and biomass. A similar scaling is used for transfers between infection levels because these are not equivalent in dimension. Thus, each specific rate for each transfer was scaled by:

for transfers up: $W_j/(W_{j+1} - W_j)$
for transfers down: $W_j/(W_j - W_{j-1})$

where W is the median value for biomass (g AFDW) in the size class, or by the ratio of parasite number between infection classes:

for transfers up: $C_k/(C_{k+1} - C_k)$
for transfers down: $C_k/(C_k - C_{k-1})$

where C is the number of cells of *P. marinus* per individual. For simplicity, these scalings are not explicitly stated in the equations given in the following sections.

THE OYSTER MODEL

The model includes parameterizations for the processes that determine the production of somatic and reproductive tissue and thus the transfer between size classes. Specifically included are formulations for: assimilated ingestion as it depends on filtration rate, ambient food supply, and assimilation efficiency; filtration rate as a function of oyster size, temperature, salinity, turbidity, and current flow; respiration as it depends upon oyster size, temperature, and salinity; the apportionment of net production into somatic and reproductive growth as a function of temperature and time of year; the preferential resorption of gonadal tissue when $NP_{j,k} < O$; and spawning as a function of the total cumulative reproductive biomass and the male/female ratio. The relationships used for these processes are shown in Table 2.

The modifications made to the oyster population model so that it could be interfaced with the *P. marinus* model consisted of including the competing effect of mussels on oyster filtration and adding sources of natural mortality for the oyster populations. Larval mortality, mortality of the postsettlement population due to predation, and mortality due to low salinity were identified as the primary sources of natural mortality other than *P. marinus*. The mussel filtration effect and mortality sources were added to the model as follows.

Mussels

Under certain conditions, mussels can be an important competitor with oysters for available food resources (Medcof 1961). The degree of competition is a complex process which depends on population density, size frequency, food content, and current flow. In the oyster model, the effect of mussels is to increase total

community filtration rate, which is used in the calculation of available food supply as described in Table 2. Available food supply is determined by the initial food content, the community demand, and the rate of food replacement by current flow. Community filtration rate, α, is calculated as:

$$\alpha = \sum_{j=1}^{11} \sum_{k=1}^{28} F_{D_{j,k}} + \sum_{i=1}^{10} Fm_{\tau_i} \quad (5)$$

where $\sum_{j=1}^{11} \sum_{k=1}^{28} F_{D_{j,k}}$ is the oyster population filtration modified by *P. marinus* as described below and $\sum_{i=1}^{10} Fm_{\tau_i}$ is the filtration of the mussel population summed over 10 mussel size classes, i, that ranged from 0 to 100 mm in 10-mm increments.

On Gulf of Mexico oyster reefs, *Brachidontes exustus* and *Brachidontes recurvus* are the principal mussel species. Few data exist for either species; therefore, the relationships used in the model to describe these species are based on those for bivalve molluscs and oysters. This approach assumes that the salinity and turbidity tolerances are somewhat similar for these co-occurring species.

Mussel weight is estimated from length using the bivalve length-to-biomass relationship given in Powell and Stanton (1985):

$$W_m = L_m^a \, 10^b \quad (6)$$

where W_m is mussel dry weight in g and L_m is mussel length in mm. Coefficient values and definitions are given in Table 3. As was done for oysters, the relationship given in Doering and Oviatt (1986) for filtration rate was used with Hibbert's (1977) biomass-to-length relationship to obtain filtration rate as a function of biomass. Hence, the mussel filtration rate equation as a function of biomass is similar to the one shown in Table 2 for oysters. The primary difference is that the ash-free dry weight, in grams, used for each mussel size class is input to the above equation to obtain mussel length, which is then input to the filtration equation.

No data exist that describe the relationship between filtration rate of *Brachidontes* and salinity. Therefore, it was assumed that the relationship is similar to that for oysters. Thus, mussel filtration rate was specified using the salinity equations given in Table 2 for oysters. This allows filtration rate to decrease as the salinity drops below 7.5 ppt and to cease at salinities below 3.5 ppt.

Brachidontes spp. are rarely important at salinities above 14 ppt (Powell unpublished data for Galveston Bay, Baughman and Baker 1949). The observations from Galveston Bay further suggest that the salinity control on mussel population density is a step function at about 14 ppt, with little further effect as salinity rises above or declines below 14 ppt. Therefore, mussel density was set to zero at salinities above 14 ppt.

Total particulate content, at high concentrations, may also reduce mussel filtration rate. Again, data sufficient to describe this for *Brachidontes* are lacking. Therefore, the relationships for oysters, which are given in Table 2, were assumed to also apply to mussels.

Oyster Mortality

While in the plankton, oyster larvae undergo considerable mortality from a variety of sources, which reduces the number of individuals that are recruited to the postsettlement population from a spawn. Oyster larval mortality was included using a linear relationship of the form:

$$\textit{number of larvae recruited spawn}^{-1} = s(\textit{number of eggs spawned}) \quad (7)$$

where s determines the rate at which individuals are lost per spawn. No attempt is made to differentiate among the many sources of planktonic mortality.

Natural mortality of the postsettlement population was also specified with a linear relationship of the form:

$$M_p = k_p(\textit{number of living oysters}) \quad (8)$$

where M_p is the number of individuals that die in a given time interval and k_p is the daily mortality rate (d^{-1}). As with larval mortality, this approach does not differentiate among the many sources of oyster mortality. For the simulations presented here, this relationship was used to produce mortality for the juvenile oyster size classes to complement the adult mortality produced by *P. marinus*.

Low salinity is a principal cause of catastrophic mortality of postsettlement oyster populations during some flood years (Hofstetter 1977, Ray 1987, Soniat and Brody 1988). Wells (1961) and Chanley (1957) provide survivorship data at low salinity for temperatures greater than 20°C, which show that salinities lower than 6 ppt produce mortality at summer temperatures and that the rate of mortality rises as salinity declines below 6 ppt. Additionally, observations given in Gunter (1953) and those from Galveston Bay (Powell unpublished data) show that oyster survivorship increases substantially at low salinity as temperature declines. Therefore, the temperature-dependent mortality produced by salinities lower than 6 ppt was modeled as:

$$M_s = k_s(\textit{number of living oysters}) \quad (9)$$

where M_s is the number dying per time and k_s in d^{-1} is given by

$$k_s = (\alpha_1 S + \beta_1)T + (\alpha_2 S + \beta_2). \quad (10)$$

Salinity, S, is given in ppt and temperature, T, is in °C. Coefficient values for the above equations are given in Table 2.

THE *PERKINSUS MARINUS* MODEL

The *P. marinus* model includes processes that govern parasite growth and mortality, those that determine the energy demand of the parasite on the host, and those that affect the physiology of the host. The relationships used to describe these processes are given in the sections that follow.

Perkinsus marinus *Growth*

Cell division time is the time between one cell division and the next for an individual cell. The population doubling time, however, depends upon the balance between the rate of cell division and the rate of cell mortality. For *P. marinus*, cell mortality is likely mediated in some way by the defense system of the oyster (Saunders et al. 1993). In the *P. marinus* population model, the biology of the parasite and the processes determining the rate of parasite division are treated separately from those that describe the oyster's defense system and the rate of parasite mortality.

Measurements of *P. marinus* division time are limited and the effects of temperature, salinity, and cell density are poorly known. However, information from Ray (1954) and Mackin and Boswell (1954) suggests that the parasite division times range from 7 to 60 hours. More recently, Choi et al. (1989) estimated a doubling time of 7 hours. The fastest rate of division, at low parasite density,

TABLE 2.

Equations and relationships used in the oyster population dynamics model. Complete discussions of these are given in Powell et al. (1992b, 1994, 1995a) and Hofmann et al. (1992, 1995).

Equations	Comments and Parameter Definitions
Filtration rate and water flow	Flow limitation on food supply is calculated using a volume of water over the bottom with length and width, L, and height, h
$\frac{\partial F}{\partial t} + \frac{\partial (uF)}{\partial x} + \frac{\partial (wF)}{\partial z} - \frac{\partial^2 (AF)}{\partial z^2} + \alpha FO = 0$	F, food u, horizontal advective velocity w, vertical advective velocity A, vertical diffusion coefficient α, total filtration rate summed over all oyster size classes, $\sum_{j=1}^{n} FR_{D,j}$ O, oyster biomass partial derivatives indicate changes in time (t) and in the horizontal (x) and vertical (z) directions
$\frac{\partial u}{\partial x} + \frac{\partial w}{\partial x} = 0$	Continuity equation
Characteristic velocity profile $u(x,z) = u_o(x)\ln(z/z_o)$	$u_o(x)$, a specific horizontal speed at height, $z = h$ z_o, bottom roughness parameter = 10% of height of oyster clumps
$u_o(x) = \hat{u}(x)/\ln(h/z_o)$	$\hat{u}(x)$, the specified speed
Food profile $F = F_o(t) + (x/L)F_1(t)$	Food assumed to be independent of height and a linear function of distance across the box. F_o, F_1 are food concentrations at the upstream and downstream boundaries of the volume of interest
Food calculation $F_o(t = 0) = F_o(t = \Delta t) = F_{oo}$	F is integrated over the volume, and the average amount of food in the box during one time step is calculated by differencing over time. F_{oo}, the specified food concentration
$F_1(t = 0) = 0$ $F_1(t = \Delta t) = F_1^1 = [-2\alpha\Delta t F_{oo} 0^\circ + (\Delta t/hL)(D^1 + D^\circ)]/$ $[1 + 0.5\alpha\Delta t 0^\circ + [(\hat{u}(L) + \hat{u}(0))(\Delta t/2L)][1 - 1/\ln(h/z_o)]]$	
Food reduction factor $F_{red} = (F_{oo} + 0.25F_1^1)/F_{oo}$	F_{red} is the fraction by which the food concentration is reduced
Food content $f^* = F_{red}F_{oo}$	f^* is the available food
Conditions for simulation	Box length, L = 1 m Thickness of bottom flow, h = 5.4 cm
Filtration rate as a function of temperature $FR_j = \frac{L_j^{0.96} T^{0.95}}{2.95}$	Filtration rate (FR_j) in ml filtered ind^{-1} min^{-1} by a particular oyster size, j; length (L_j) obtained from W_j, the ash-free dry weight in **g**; T, temperature
$L_j = W_j^{0.117} 10^{0.669}$	
Filtration rate as a function of ambient salinity, S	
$FR_{s_j} = FR_j$	at $S \geq 7.5$ ppt
$FR_{s_j} = FR_j(S - 3.5)/4.0$	at $3.5 < S < 7.5$ ppt
$FR_{s_j} = 0$	at $S \leq 3.5$ ppt
Filtration rate as a function of turbidity	Calculated similarly to f^*
$\tau^* = \tau_{red}\tau_{oo}$	τ, total particulate content (inorganic + organic) in g l^{-1}; x, the percent reduction in filtration rate
$\tau = (4.17 \times 10^{-4})(10^{0.0418x})$	Filtration rate with turbidity effects
$FR_{\tau_j} = FR_{s_j}\left[1 - 0.1\left(\frac{\log_{10}\tau + 3.38}{0.0418}\right)\right]$	
Ingestion $I_{j,k} = f^* FR_{D_{j,k}}$	Ingestion rate (I) as a function of food concentration and filtration rate
Assimilation $A_{j,k} = I_{j,k}A_{eff}$	A_{eff}, assimilation efficiency
Respiration as a function of temperature $R_j = (69.7 + 12.6T)W_j^{b-1}$	Respiration rate (R_j) for a particular oyster size class in μl O_2 consumed hr^{-1} g dry wt^{-1}; b = 0.75
Respiration as a function of salinity $R_r = 0.007T + 2.099$	at $T < 20$°C

TABLE 2.

continued

Equations	Comments and Parameter Definitions
$R_r = 0.0915T + 1.324$	at $T \geq 20$°C
$R_{T_j} = R_j$	at $S \geq 15$ ppt
$R_{T_j} = R_j/(1 + [(15 - S)(R_r - 1)/5])$	at 10 ppt $< S <$ 15 ppt
$R_{T_j} = R_j R_r$	at $S \leq 10$ ppt
Reproduction, R_f:	
Juvenile/adult boundary	0.39 g ash-free dry weight; about 50 mm
$Pr_{j,k} = R_{\text{eff}_j} NP_{j,k}$	Reproductive tissue development for a given oyster size class as a function of reproductive efficiency, R_{eff_j}, and total net production, $NP_{j,k}$
$R_{\text{eff}_{j,k}} = 0.054T(t) - 0.729$	Reproductive efficiency temperature dependence for January to June
$R_{\text{eff}_{j,k}} = 0.047T(t) - 0.809$	Reproductive efficiency temperature dependence for July to December
when $NP_{j,k} < 0$	Preferential resorption of gonadal tissue
$R_{f_{j,k}} = 0.20\, O_{j,k}$	Spawning occurs when the reproductive biomass exceeds 20% of total oyster biomass
$f_{\text{ratio}} = 0.021\, L_b - 0.62$	f_{ratio}, the ratio of females to males; L_b, length in mm
number of eggs spawned $= R_{f_{j,k}} \left(\frac{1}{C}\right) \left(\frac{1}{W_{\text{egg}}}\right)$	Number of eggs spawned, C is number of calories per egg, W_{egg} is egg weight
$W_{\text{egg}} = 2.14 \times 10^{-14}\, V_{\text{egg}}$	V_{egg}, oyster egg volume
Larval recruitment	Larval planktonic time assumed to be 20 days
Larvae mortality	
Number of larvae recruited spawn^{-1} $= s$ (number of eggs spawned)	s, the mortality rate, in spawn^{-1}
Postsettlement population natural mortality	
$M_p = k_p$(number of living), for $j = k,l$	M_p, the number dying time^{-1} k_p, the daily mortality rate (d^{-1}); k and l, the inclusive size classes being affected by mortality
Postsettlement salinity mortality	
$M_s = k_s$ (number of living)	M_s, the number dying time^{-1}
$k_s = (\alpha_1 S + \beta_1)T + (\alpha_2 S + \beta_2)$	K_s, daily mortality rate (d^{-1}) $\alpha_1 = -0.000348$ $\alpha_2 = 0.00232$ $\beta_1 = 0.01764$ $\beta_2 = -0.3089$ S, ambient salinity (ppt) T, ambient temperature (°C)
Caloric conversions	
Oysters	6100 cal (g dry wt)$^{-1}$
Food	5168 cal (g dry wt)$^{-1}$
Oyster eggs	6133 cal (g dry wt)$^{-1}$

observed by Saunders et al. (1993) ranged between 4 and 10 hours at 30°C and 17 ppt.

Given the limited observations on *P. marinus* growth *in vivo*, this process was modeled using standard relationships for temperature and salinity dependencies which were calibrated by comparing the simulated growth of *P. marinus* to data sets that provide observations of the seasonal dependency of parasite infection intensity as salinity and temperature change. These data came from April Fools Reef in Galveston Bay, TX (Soniat 1985), Biloxi Bay, MS (Ogle and Flurry 1980), and North Inlet, SC (Crosby and Roberts 1990).

Temperature control on the specific rate of parasite division, $r_d(T)$, was assumed to follow a standard exponential form:

TABLE 3.

Coefficient definitions and values for the mussel model.

Coefficient	Definition	Value	Units
Fm_τ	Mussel filtration rate	Calculated	ml mussel^{-1} min^{-1}
W_m	Mussel weight	Calculated	g dry wt
L_m	Mussel length	Assigned	mm
a	Mussel weight scaling factor	−4.8979	No units
b	Mussel weight scaling factor	2.8734	No units

$$r_d(T) = r_{d0}\, e^{\alpha(T(t) - T_0)}. \quad (11)$$

To calibrate equation (11), a known division rate at a given temperature is needed. Observations of field populations suggest that infection intensity begins to rise in most populations when the temperature exceeds 20°C and the salinity exceeds 20 ppt. Therefore, the 20°C–20 ppt boundary was used to standardize parasite division and mortality rates. At 20°C and 20 ppt, parasite division should just balance loss (Ray 1954, Mackin 1962, Andrews 1988). The division time at 20°C and 20 ppt was set at 30 hours by comparing simulated distributions to those in Soniat (1985), Ogle and Flurry (1980), and Crosby and Roberts (1990). This division time is within the ranges of those reported from the limited laboratory and *in vivo* measurements. A Q_{10} of 2.0, which is consistent with measurements for *P. marinus* (Chu and Greene 1989), is used to calculate a parasite division rate at temperatures other than 20°C. The coefficients and their values thus determined for equation (11) are defined in Table 4.

The rate of parasite division is independent of salinity except at and below 10 ppt (Chu and Greene 1989, Ragone and Burreson 1993). Thus, for salinities (S) below 10 ppt, equation (11) is modified as:

$$r_d(T,S) = r_{d1} \left(\frac{S}{10}\right) e^{\alpha(T(t) - T_0)} \quad (12)$$

where coefficient definitions and values are given in Table 4. This relationship provides a decrease in parasite division rate at low salinity but retains the temperature relationship.

Simulations of *P. marinus* population dynamics using equation (12) in the oyster–*P. marinus* model resulted in parasite growth rates and densities that were too high relative to those suggested by field measurements in Soniat (1985), Ogle and Flurry (1980), and Crosby and Roberts (1990) under the appropriate environmental constraints (Hofmann et al. 1995). Most measurements of protozoa in culture show that parasite division rate decreases at high population densities as food becomes limiting (Hall 1967). A similar response by *P. marinus* is suggested by *in vivo* experiments in which the rate of DNA production by *P. marinus* at various parasite densities declined at high densities (Saunders et al. 1993). Also, a decrease in hemolymph protein in oysters has been noted during summer months when *P. marinus* infection intensity is high (Chintala and Fisher 1991) and as a result of MSX infection (Ford 1986). Using the measurements from Saunders et al. (1993), an

TABLE 4.

Coefficient definitions and values for the *P. marinus* population model.

Coefficient	Definition	Value	Units
$r_d(T)$	Specific rate of parasite division	Calculated	d^{-1}
r_{d0}	Base specific parasite division rate	0.555	d^{-1}
α	Q_{10} conversion	0.06931	$°C^{-1}$
T_0	Base temperature for parasite division rate	20	°C
S_0	Base salinity for parasite division rate	20	ppt
r_{d1}	Base specific parasite division rate	0.555	d^{-1}
β	Parasite density scaling factor	2.454×10^8	g AFDW $cell^{-1}$
C_k	Parasite number	Calculated	Number of cells
W_j	Oyster weight	Table 1	g AFDW
γ	Parasite density scaling factor	−1.5	No units
$r_m(T,S)$	Specific parasite loss rate	Calculated	d^{-1}
r_{m0}	Base specific parasite loss rate	0.555	d^{-1}
δ	Q_{10} conversion	0.08153	$°C^{-1}$
Ec	Total *P. marinus* energy demand	Calculated	cal d^{-1}
Eg	Energy for *P. marinus* population increase	Calculated	cal d^{-1}
Er	Energy for *P. marinus* respiration demand	Calculated	cal d^{-1}
El	*P. marinus* mortality	Calculated	cal d^{-1}
ϵ	Conversion	1.16×10^4	hr cal d^{-1} nl^{-1}
D	Average parasite cell diameter	8	μm
ζ	Conversion	9.57×10^{-10}	cal μm^{-3}
ω	Respiration scaling factor	−4.09	ml hr^{-1} μm^{-3}
θ	Respiration scaling factor	0.75	No units
κ	Filtration scaling factor	0.58	No units
λ	Filtration scaling factor	579	No units
μ	Conversion	-2.287×10^{-4}	g AFDW $cell^{-1}$
$FR_{D_{j,k}}$	Filtration rate, infected oyster	Calculated	ml $oyster^{-1}$ min^{-1}
C_{L_j}	Lethal parasite density	Calculated	Cells $oyster^{-1}$
ν	Mortality scaling factor	2.057	No units
z	Weight scaling factor	1.3258×10^{-7}	g AFDW
q	Weight scaling factor	0.2625	No units
σ	Mortality scaling factor	3.2	No units
υ	Weight conversion factor	5	g wet wt (g dry wt)$^{-1}$
τ	Infection level scaling factor	1409.9	Cells (g wet wt)$^{-1}$
ϕ	Infection level scaling factor	0.64296	No units
r_t	Specific rate of transmission	Calculated	d^{-1}
r_{tb}	Base specific interpopulation transmission rate	0.2	y^{-1}
r_{t0}	Base specific intrapopulation transmisson rate	12	y^{-1}

empirical relationship that modifies the specific parasite division rate at high parasite density, $r_d(\rho)_{j,k}$, was derived as:

$$r_d(\rho)_{j,k} = \beta r_d(T,S)\left(\frac{C_k}{W_j}\right)^{\gamma} \quad (13)$$

where $r_d(T,S)$ is determined from equation (12). Coefficient definitions and values are given in Table 4. In the model, the parasite division rate that is used is the minimum of that determined from equations (12) and (13).

Perkinsus marinus *Mortality*

Mortality of *P. marinus* is presumably a result of the oyster defense system response. Thus, parasite mortality was parameterized using data obtained for hemocytes, which are an important component of the oyster's defense mechanism (Fisher 1988). These data show that parasite mortality is temperature and salinity dependent. Moreover, field (Soniat 1985, Burrell et al. 1984) and laboratory (Fisher et al. 1992) observations show that the effect of salinity on parasite mortality is discernible only at high temperatures. One explanation for this is that hemocytes are already maximally active at low temperature so that salinity changes have little effect. However, at higher temperatures where hemocyte activity is reduced, some capability is recovered when the oyster is exposed to low salinity. Thus, a temperature- and salinity-dependent relationship for the specific parasite mortality rate, $r_m(T,S)$, was obtained using measurements of hemocyte activity reported in Fisher and Newell (1986), Fisher and Tamplin (1988), Fisher et al. (1989, 1992), and Chintala and Fisher (1991) as:

$$r_m(T,S) = r_{m0}\, e^{-\delta\left(\frac{S(t)}{S_0}\epsilon\right)}\, e^{-\delta\left(\frac{T_0-10}{S_0}\right)(S(t)-S_0)}. \quad (14)$$

where ϵ is the larger of the temperatures at 10°C or the difference between the ambient temperature and the base temperature of 20°C, i.e., $\max(10°C, T(t) - T_0)$. The definitions and values for the coefficients in the above equation are given in Table 4. The value used for δ was obtained by applying a Q_{10} of 2.26 to the base mortality rate. The specific parasite mortality rate assumes no reduction in hemocyte activity at extreme low salinity. Ford and Haskin (1988) found active hemocytes down to 6 ppt, and oyster mortality from low salinity begins at lower salinities.

As with parasite division, mortality should also be dependent on parasite density. As parasite density increases, the effectiveness of the defense system should decrease. Anderson et al. (1992) showed that the number of hemocytes in heavily infected oysters is only about double that in lightly infected oysters, whereas the number of *P. marinus* cells is a factor of 1000 or more higher. Thus, the relative activity of the hemocytes must decline at high parasite density. Measurements sufficient to exactly describe the relationship between parasite concentration and mortality are not available. Hence, the parasite density effect on mortality rate was assumed to follow the same relationship as was used for the parasite density effect (equation 13) on parasite division rate:

$$r_m(\rho)_{j,k} = \beta r_m(T,S)\left(\frac{C_k}{W_j}\right)^{\gamma}. \quad (15)$$

Coefficient definitions and values are given in Table 4. The specific parasite mortality rate was taken to be the minimum of the rate calculated using equations (14) and (15). It is assumed that no *P. marinus* mortality occurs as a direct result of extremes in temperature and salinity. Available data suggest that *P. marinus* is as resistant to environmental extremes as its oyster host (Goggin et al. 1990) and calibrating simulations of *P. marinus* growth against existing data sets did not require an additional mortality source beyond that provided by the host's defense system (Hofmann et al. 1995).

Perkinsus marinus *Energy Demand*

The *P. marinus* population depends on the oyster host to provide sufficient energy to support parasite respiration and growth. Thus, the energy requirement of the parasite population, *Ec*, can be expressed as:

$$Ec = Eg + Er - El \quad (16)$$

where *Eg* is the energy required to increase the population biomass through parasite division and *Er* is the energy requirement for population respiration. The last term on the right of equation (16), *El*, represents the return of energy to the host from the parasite which occurs through parasite mortality. Although hemocyte exomigration (Cheng 1983) might limit the importance of *El*, exomigration is not included in the model. The terms in the above equation are formulated as described below.

The energy requirement for population growth is defined by *Eg* − *El* and is determined by the net change in parasite number ($C_{j,k}$) in the *P. marinus* population in a specific time interval. This is calculated from the difference in the specific parasite division and mortality rates as:

$$\frac{dC_{j,k}}{dt} = (r_d(\rho)_{j,k} - r_m(\rho)_{j,k})\, C_{j,k}. \quad (17)$$

The change in parasite number in a time interval, $\Delta C_{j,k}$, obtained from the above equation is converted to calories exchanged between the parasite and its host by:

$$Eg_{j,k} - El_{j,k} = \epsilon\, V\, \Delta C_{j,k} \quad (18)$$

where ϵ is a conversion factor obtained by assuming that 5 g wet weight is equivalent to 1 g dry weight and that 20 joules is equivalent to 1 mg dry weight (Laybourn-Parry 1987). Parasite cell volume, *V*, is calculated as:

$$V = \frac{4}{3}\pi\left(\frac{D}{2}\right)^3. \quad (19)$$

The average cell diameter, *D*, is from Ray (1954). Coefficient values and definitions are given in Table 4.

The respiratory energy required by the *P. marinus* population is obtained from:

$$Er_{j,k} = \zeta\, e^{(\alpha(T(t)-T_{30})}\, 10^{\omega} V^{\theta} C_{j,k} \quad (20)$$

where the conversion factor, ζ, assumes 4.83 ml O_2 per calorie (Powell and Stanton 1985). The exponents ω and θ, which scale respiration rate to parasite cell volume, are from measurements made for protozoa (Fenchel and Finlay 1983). The value for α assumes a Q_{10} of 2 (Laybourn-Parry 1987). The effect of salinity on *P. marinus* respiration rate is unknown and therefore is not included. Coefficient values and definitions are given in Table 4.

Effects of* Perkinsus marinus *on Oyster Physiology

The primary effects of *P. marinus* infection on oysters are to reduce oyster filtration rate (Lund 1957) and eventually cause host mortality. Although increased predation is frequently described as a product of parasitism (Jakobsen et al. 1988, Hadeler and Freed-

man 1989, Schmid-Hempel and Schmid-Hempel 1988), no evidence exists for selective predation of *P. marinus*–infected individuals. Thus, selective predation is not included in the model. Also, the possible loss of *P. marinus* during spawning (Dungan and Roberson 1993) is not included.

Mackin and Ray (1955) provide measurements of *P. marinus* that can be used to derive a relationship that describes the reduction in oyster filtration rate with infection intensity. These measurements show an exponential decrease in oyster filtration rate that depends on the ratio of the number of cells of the parasite to the size (weight) of the host. This reduction in filtration can be expressed as:

$$Dred_{j,k} = \frac{\kappa}{\lambda e^{\mu \frac{C_k}{W_j}} + 1} \tag{21}$$

Coefficient definitions and values are given in Table 4. The expression given in equation (21), when applied to the oyster filtration rate, FR_{τ_j}, defined in Table 2, results in a fractional reduction in filtration rate as:

$$FR_{D_{j,k}} = FR_{\tau_j}(1 - Dred_{j,k}) \tag{22}$$

where $FR_{D_{j,k}}$ is the filtration rate that results when the oysters are infected with *P. marinus*.

The level of *P. marinus* infection in an oyster population is typically diagnosed in terms of a 0- to 5-point scale that was developed by Mackin (1962), with 5 being the heaviest infection level. Field and laboratory measurements show that oyster mortality generally occurs in individuals that have an infection intensity that corresponds to a 5 on this scale (Andrews 1988). Populations with mean infection intensities of 3 or more generally suffer 50 to 75% mortality per year (Ray and Chandler 1955, Mackin 1961, Mackin and Hopkins 1961). These observations provide a basis for determining the lethal *P. marinus* infection level in the simulated oyster populations.

A relationship was developed between host mortality, host size, and *P. marinus* number by assuming that host mortality occurs when the energy demand of the *P. marinus* population is some fraction of the host's net production. This relationship is based on net production values calculated for uninfected oysters as described by White et al. (1988) and is of the form:

$$\frac{2NP_{w_j}}{Ec} = C_{L_j} \tag{23}$$

where NP_{w_j} is net production, Ec is the caloric requirement of the *P. marinus* population as determined from equation (14), and C_{L_j} is the lethal parasite density (cells oyster^{-1}) for any oyster size class, j.

The above equation allows for a size dependency in lethal parasite density that is suggested by measurements given in Choi et al. (1989) and is consistent with a size-dependent scope for growth in oyster populations (Hofmann et al. 1992). The factor of 2 used in equation (21) was determined empirically by using yearly mortality rates of 90, 50, and 10% for the market-size population and comparing the resulting simulated populations with oyster populations reported in the field studies by Ogle and Flurry (1980), Soniat (1985), and Crosby and Roberts (1990).

The lethal parasite density from equation (23) can then be related to oyster size through a regression of the form:

$$C_{L_j} = 10^{\left(\nu \log_{10}\left(\left(\frac{W_j}{z}\right)^q + \sigma\right)\right)} \tag{24}$$

Note that because equation (24) is obtained from a regression, the units on the two sides of the equation are not equivalent. Coefficient definitions and values are given in Table 4.

Assuming that *P. marinus* infections are initiated by one cell, then depending on oyster size, 22 to 27 population doublings are needed to reach the lethal density. Smaller oysters require fewer population doublings to reach the lethal parasite level. As required by field observations, the above equation yields a value of 5 on Mackin's Scale when converted according to Choi et al. (1989) as:

$$C_{L_j} = \upsilon\tau(10^{\phi M})W_j \tag{25}$$

where M is the Mackin's Scale infection intensity as defined by Craig et al. (1989). Coefficient values and definitions are given in Table 4.

Equation (24) is consistent with the suggestion that oyster mortality could be at least partly explained by a negative energy budget produced when the energy demand of *P. marinus* exceeds the assimilation rate of the oyster (Choi et al. 1989). However, the exact mechanism by which *P. marinus* causes mortality of the oyster host is unknown, and some studies have reported significant effects on the host at lower infection levels (e.g., Paynter and Burreson 1991). The justification for using the approach given above comes from favorable comparisons between simulated and observed levels of *P. marinus* infection under equivalent environmental conditions (Hofmann et al. 1995).

Perkinsus marinus *Transmission*

The available studies of the transmission of *P. marinus* indicate that oyster density and distance between infected host populations affect the rate of infection (Andrews and Ray 1988, Ford 1992, Mackin 1952). However, little information on the transmission of this disease from controlled experiments is available (Andrews 1965, 1988). Therefore, the transmission of *P. marinus* was modeled using general relationships for disease transmission. These formulations were then calibrated against field data.

The specific rate of infection of uninfected oyster individuals, r_t, was assumed to be the result of an interpopulation transmission rate, r_{tb}, and an intrapopulation specific transmission rate, r_{t0}, as:

$$r_t = r_{tb} + r_{t0}\left(\frac{P_1 + P_2 + P_3}{3}\right) \tag{26}$$

where P_1, P_2, and P_3 are factors that modify the intrapopulation transmission rate.

Insufficient data were available to include the expected relationship between oyster filtration rate and *P. marinus* transmission rate as occurs in other host-parasite systems (e.g., Gee and Davey, 1986). This effect could be important at higher latitudes where filtration ceases during the winter, thus limiting transmission rate. However, the decrease in *P. marinus* prevalence and infection intensity produced by the effects of low temperature on parasite growth and mortality, that occur during the winter, should minimize any error due to exclusion of this effect. Also, a suspected influence of salinity on *P. marinus* transmission rate (Paynter and Burreson 1991, Chu and La Peyre 1993) is not included in the model.

The interpopulation infection intensity was determined by using observations from San Antonio Bay, TX, obtained as part of the NOAA National Status and Trends program. A catastrophic

flood produced 100% mortality of oysters in this bay in 1988. As the bay recovered, the infection intensity and prevalence of *P. marinus* were monitored in the oyster population. These observations showed that *P. marinus* infection returned to regional norms in about 2 years. Simulations of this event required an interpopulation infection intensity (r_{ib}) of 0.2 y^{-1}. Field experiments by Paynter and Burreson (1991) yielded similar results.

Three variables—oyster density, *P. marinus* prevalence, and *P. marinus* infection intensity—were used to determine the intrapopulation transmission rate. Factors affecting the intrapopulation transmission rate were formulated as follows. The prevalence of infection in a population varies between 0 and 1, where 0 represents an uninfected population and 1 represents a population in which all individuals are infected. At each time step in the model the fraction of the total population that was infected with *P. marinus* was calculated and this value was used to specify P_1 as:

$$P_1 = \textit{fraction infected} \tag{27}$$

Mean population infection intensities of 3.5 and above on Mackin's Scale are associated with substantial oyster mortality. Mortality should maximize transmission rate by releasing infective elements into the water column where they are transmitted to other individuals. Thus, P_2 was specified by establishing a ratio between the total parasite density, *TCD*, in the simulated oyster population and the parasite density that corresponds to an infection level (*IL*) of 3.5. Limiting the maximum value of this ratio to 1 yields a maximum transmission rate at all population infection intensities ≥3.5 of:

$$P_2 = \min\left(1., \frac{TCD}{IL}\right) \tag{28}$$

where

$$TCD = \frac{\Sigma_{k=1}^{28} C_k}{\Sigma_{j=1}^{11} = O_j v} \tag{29}$$

and *IL* corresponds to 2.5×10^5 cells (g wet wt)$^{-1}$.

The proximity of oyster individuals to one another also affects the rate of disease transmission. This effect is included by comparing the total simulated oyster population density with a relatively high oyster population density and limiting this value to a maximum of 1 as:

$$P_3 = \min\left(1., \sum_{j=1}^{11}\sum_{k=1}^{28} \frac{O_{j,k}}{OD}\right) \tag{30}$$

where *OD* is 4000 oysters m^{-2} (May 1971, Dame 1976).

A dense, heavily infected population [$(P_1 + P_2 + P_3)/3 = 1$] should produce an intrapopulation transmission rate that is capable of infecting all uninfected individuals within 6 months. To achieve this effect, the maximum intrapopulation transmission rate (r_{i0}) was set to 12 y^{-1}.

Model Implementation

The oyster and *P. marinus* model described above requires input of environmental measurements that describe ambient food supply, turbidity level, current flow velocity, salinity, and temperature conditions. For this study, time series of these data were constructed to illustrate specific environmental effects. In all cases, the structure of the environmental time series was based on measurements made in Galveston Bay, TX. The time series consist of monthly averaged values that extended for 1 year. The various environmental time series are given in Table 5. The specific combination of the environmental series for the different simulations is given in Table 6.

The oyster population–*P. marinus* model was solved numerically using an implicit (Crank-Nicolson) tridiagonal solution technique with a 1-day time step. All simulations began on January 1 (Julian day 1) and ran for 6 years. This amount of time was sufficient for the oyster and parasite population to adjust to the environmental forcing. Each simulation was initialized with an oyster size-frequency distribution obtained from a reef, South Deer Island, in the West Bay section of Galveston Bay, TX, in spring 1992 (Fig. 3). The initial density of the individuals in the oyster population was set at 20 individuals m^{-2}. The mussel size-frequency distribution used in the model is also from Galveston Bay, TX, and is given in Table 5. Initially, *P. marinus* was specified to be at 50% prevalence in each oyster size class. This allowed the simulated populations to more rapidly come into equilibrium with environmental conditions than would occur using 0 or 100% prevalence.

The simulated distribution of *P. marinus* in the oyster population depends on the rate of larval recruitment and juvenile mortality because new recruits, being uninfected, reduce prevalence and population infection intensity. In most of the simulations, obtaining *P. marinus* prevalence and infection intensities that were comparable to observed values required a larval survivorship of 1 individual in 10^8 larvae spawned and an independent (non–*P. marinus*) source of juvenile mortality yielding a 1% survivorship the first year after settlement. Both survivorship rates are typical of those reported for bivalves (Brousseau et al. 1982, Powell et al. 1984, Cummins et al. 1986). Other survivorship rates were used as indicated in Table 6.

MECHANISMS FOR STARTING AN EPIZOOTIC

A Growing, Parasitized Oyster Population

The first simulation with the oyster-parasite model was designed to provide a reference against which simulations considering factors that produce epizootics can be compared. The reference simulation was configured to represent conditions in Galveston Bay, TX. Galveston Bay supports a substantial oyster fishery in most years and is currently in a phase of significant oyster reef expansion (Powell et al. 1995b). Food supply throughout the bay is adequate to support the present oyster population; however, a 15% decrease in food supply would restrict population growth (Powell et al. 1995a). Other environmental factors, such as temperature and salinity, are usually within ranges that are conducive to oyster growth to market size (76 mm). The specific conditions used for the reference simulation are given in Tables 5 and 6.

P. marinus prevalence in Galveston Bay oyster populations normally exceeds 90% (Powell et al. 1992a), and significant yearly *P. marinus*–produced mortality, frequently in excess of 50% of the market-size portion of the population, can occur. However, epizootics rarely occur and oyster populations normally exist in quasiequilibrium with *P. marinus* such that prevalence remains high and mortality remains moderate. Hence, limitations on growth of the oyster population tend to be from *P. marinus*–induced disease, the vagaries of larval survival, and predators such

TABLE 5.

Environmental time series used as input to the oyster population–*P. marinus* model.

Food Supply Time Series (mg l^{-1})											
Summer bloom (SB)—after Hofmann et al. (1992)											
Jan	Feb	Mar	Apr	May	June	July	Aug	Sep	Oct	Nov	Dec
0.50	0.50	0.75	0.75	1.25	1.25	1.25	1.25	0.75	0.75	0.50	0.50
Summer bloom—reduced winter food (LW)											
Jan	Feb	Mar	Apr	May	Jun	Jul	Aug	Sep	Oct	Nov	Dec
0.25	0.25	0.75	0.75	1.25	1.25	1.25	1.25	0.75	0.75	0.25	0.25
Summer bloom—reduced summer food (LS)											
Jan	Feb	Mar	Apr	May	Jun	Jul	Aug	Sep	Oct	Nov	Dec
0.50	0.50	0.75	0.75	1.00	1.00	1.00	1.00	0.75	0.75	0.25	0.25
Summer bloom—increased summer food (HS)											
Jan	Feb	Mar	Apr	May	Jun	Jul	Aug	Sep	Oct	Nov	Dec
0.50	0.50	0.75	0.75	2.00	2.00	2.00	2.00	0.75	0.75	0.50	0.50
Turbidity Time Series (g l^{-1})											
High-turbidity event (HT)											
Jan	Feb	Mar	Apr	May	Jun	Jul	Aug	Sep	Oct	Nov	Dec
0.00	0.00	0.00	0.00	0.01	0.01	0.01	0.01	0.00	0.00	0.00	0.00
Current Speed Time Series (cm s^{-1})											
Low-flow event (LF)											
Jan	Feb	Mar	Apr	May	Jun	Jul	Aug	Sep	Oct	Nov	Dec
1.0	1.0	1.0	1.0	0.001	0.001	0.001	0.001	1.0	1.0	1.0	1.0
Salinity Time Series (ppt)											
High-salinity event (Hsal)											
Jan	Feb	Mar	Apr	May	Jun	Jul	Aug	Sep	Oct	Nov	Dec
20	20	20	35	35	35	35	35	35	20	20	20
Low-salinity event (Lsal)											
Jan	Feb	Mar	Apr	May	Jun	Jul	Aug	Sep	Oct	Nov	Dec
20	20	20	10	10	10	10	10	10	20	20	20
Low-salinity event (Lrsal)											
Jan	Feb	Mar	Apr	May	Jun	Jul	Aug	Sep	Oct	Nov	Dec
20	20	20	15	15	15	15	15	15	20	20	20
Temperature Time Series (°C)											
Galveston Bay, Texas (GB)											
Given in Dekshenieks et al. (1993)											
High winter temperature (Ht)											
Winter temperatures (October to March) are 2°C higher than those measured in Galveston Bay											
Low winter temperature (Lt)											
Winter temperatures (October to March) are 2°C lower than those measured in Galveston Bay											
Oyster Abundance—Confederate Reef											
Size (upper size limit in mm)											
25.	35.	50.	63.5	70.	76.	88.9	100.	110.	125.	150.	
Abundance (number m^{-2})											
1.8	2.0	4.8	4.6	2.4	1.6	2.2	0.8	0.4	0.2	0.0	
Mussel Abundance											
Size (upper size limit in mm)											
10.	20.	30.	40.	50.	60.	70.	80.	90.	100.		
Abundance (number m^{-2})											
50	50	50	50	0	0	0	0	0	0		

as crabs and oyster drills (Powell et al. 1995a), which represent top-down controls, as defined by Hunter and Price (1992).

Environmental conditions that are typical of high-salinity reefs in Galveston Bay, TX, result in the simulated oyster population shown in Figure 4. A relatively stable market-size population is maintained over 5 years (Fig. 4A) and the submarket-size component (not shown) of the population rises gradually during the first 4 years and more rapidly thereafter. A decline in year 6 is produced by high population densities exceeding the available food supply. The biomass-to-length conversion given in Table 1 was used to calculate the number of market-size individuals. This relationship is representative of Galveston Bay oyster reefs, although substantial variation exists within the bay (Powell unpublished data). Minor mortality events, due to *P. marinus*, occur during the summer of the second and fourth years (Fig. 4A). The large decrease in oyster abundance seen at the end of 6 years results from the effects of crowding caused by significant population expansion in years 5 and 6 (see Powell et al. 1994 for a discussion). The oyster population maintains reproductive capability throughout the simulation, with spawning occurring throughout much of the late spring and summer (Fig. 4B) in each year.

TABLE 6.

The combination of environmental time series given in Table 5 and additional parameter values used for the simulations. *The different environmental time series are defined as: summer bloom (SB), summer bloom with reduced winter food (LW), summer bloom with reduced summer food (LS), summer bloom with increased summer food (HS), high-salinity event (Hsal), low-salinity event (Lsal), low-salinity event with slightly higher summer values (Lrsal), high-turbidity event (HT), low-current-flow event (LF), high winter temperatures (Ht), and low winter temperatures (Lt). The *P. marinus* division time and juvenile oyster mortality used in each simulation are also shown. Except where indicated, juvenile survival was 1 in 10^8. Values indicate a 12-month continuous time series at that level.

Figure Number	Salinity (ppt)	Temperature (°C)	Food	Turbidity (g l^{-1})	Flow (cm s^{-})	Halving Time (hours)	Juvenile Mortality (d^{-1})	Comments
4	20	GB	SB	0	1.0	60	0.0064	
5	20	GB	SB/LW /SB	0	1.0	60	0.0064	Time series split 1/1/4
6	20	GB	SB/LS /SB	0	1.0	60	0.0064	Time series split 1/1/4
7	20	GB	SB	0/HT /0	1.0	60	0.0064	Time series split 1/1/4
8	20	GB	SB	0	1.0/LF /1.0	60	0.0064	Time series split 1/1/4
9	20	GB	SB	0	1.0	60	0.0064	Mussels present days 450–650
10	20/Hsal /20	GB	SB	0	1.0	60	0.0064	Time series split 1/1/4
11	20/Lsal /20	GB	SB	0	1.0	60	0.0064	Time series split 1/1/4
12	20/Hsal /20	GB/Ht /GB	SB	0	1.0	60	0.0064	Time series split 1/1/4
13	20	GB	SB	0	1.0	120	0.0064	
14	20	GB	SB/LS/ HS/SB	0	1.0	60	0.0064	Time series split 1/1/1/3
15	20/Hsal/ Lrsal/20	GB/Ht/ LT/HB	SB	0	1.0	60	0.0064	Time series split 1/1/1/3
16	20	GB	SB	0	1.0	60	0.0064	Summer recruitment rate: year 2, 1 in 10^9; year 3, 6 in 10^9

One of the checks on the simulation is to ensure that the simulated seasonal progression of *P. marinus* infection intensity and prevalence corresponds to measured patterns. The observed pattern of *P. marinus* prevalence in oyster populations usually shows lows in late winter to early spring, an increase in late spring, and a peak in mid to late summer. The pattern of prevalence for the total simulated oyster population (Fig. 4C, solid line) shows lows in the summer and highs in the winter, which is exactly the opposite of field measurements. The lows in prevalence in the simulated populations occur during recruitment following major spawning events.

The standard approach for measuring *P. marinus* prevalence involves the collection of the largest individuals in the population, normally those of market size. If only this portion of the simulated oyster population is considered, prevalence exceeds 80% in most months of the year (Fig. 4C, dotted line). Lows occur in fall and winter as submarket-size adults grow to market size, but prevalence does not decline to the normally measured winter levels. Recent experimental studies (Choi et al. 1989) have shown that the thioglycollate technique typically used to assess *P. marinus* prevalence (Ray 1966) frequently misdiagnoses light infections as negative. Thus, if it is assumed that infections of $\leq 2^{12}$ cells ind^{-1} are normally misdiagnosed as negative, then the pattern of prevalence in the market-sized portion of the simulated oyster populations shows the observed seasonal cycle (Fig. 4C, dashed line). Low prevalences occur in February and March, when many false negatives are reported, and peak prevalences occur in the late summer.

A similar problem exists for the calculation of mean infection intensity for the population depicted in Figure 4B when using Mackin's (1962) Scale as modified by Craig et al. (1989). The simulated seasonal progression of infection intensity matches the observed pattern only when the market-sized portion of the population is considered (Fig. 4B, dotted line). The seasonal cycle of infection intensity in the entire population (Fig. 4B, solid line) can be discerned but summer highs are depressed as disease intensification in the adults is offset by recruitment of uninfected individuals. Thus, the seasonal cycle that is observed in *P. marinus* prevalence and infection intensity is dependent upon the size class structure of the sampled population. The routine sampling of only the largest individuals in the population normally does not accurately portray the disease status of the entire population. The implications of this are discussed more fully in Hofmann et al. (1995).

The level of *P. marinus* prevalence that occurs in the simulated oyster populations shown in Figure 4 in response to Galveston Bay environmental conditions remains above 60% throughout most of the year. Yearly highs exceed 90% in most years. Mean infection intensity of the market-size adults reaches 4 on Mackin's Scale in years when mortality occurs. Infection intensity in the entire oyster

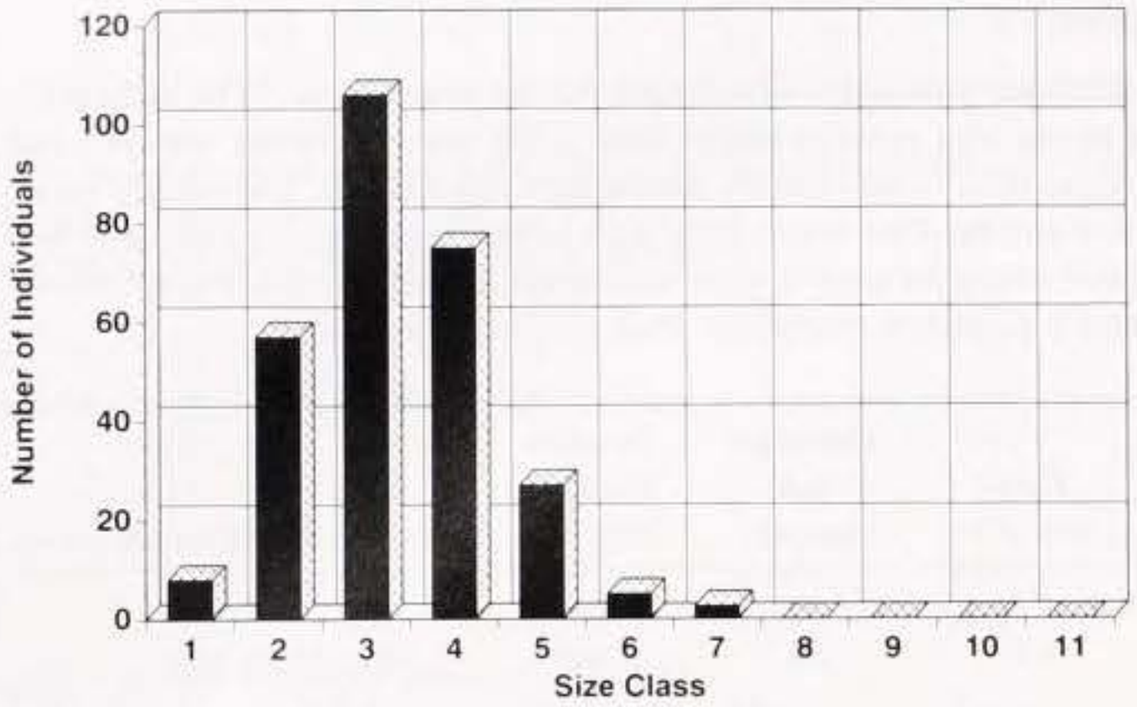

Figure 3. Size-frequency distribution of oysters that was used to initialize the oyster population model. Data are from observations made at South Deer Island in the West Bay section of Galveston Bay, TX, in spring 1992.

population averages 2 to 3, a light to moderate infection, during the summer and fall. This is lower than that for the market-size population due to the dilution effect of new recruits. The infection intensity for the entire oyster population drops to about 1 during the winter. This is higher than the infection level in the market-size fraction of the populations because the newly recruited smaller individuals, with the same number of *P. marinus* cells, have higher infection intensities on a cell per gram basis.

Infection intensity in the market-size individuals is about 3.5 on Mackin's Scale (moderate infections) in most years. However, in years in which there is significant *P. marinus* mortality, infection intensity nears 4 on Mackin's Scale. This small variation in infection intensity, which corresponds to about 1 to 2 population doublings (Hofmann et al. 1995), is all that is required to separate years of moderate-to-low mortality from years having significant mortality events.

TRIGGERING MECHANISMS FOR EPIZOOTICS

Rapid growth and high fecundity are the principal defenses against predation and disease for many host-prey/parasite-predator systems (e.g., Onstad and Maddox 1989, Warburton 1958). Oyster populations are no exception, with recruitment, growth, and fecundity usually exceeding, by some small amount, the combined rate of *P. marinus* transmission, intensification, and mortality. Therefore, mechanisms that can potentially trigger epizootics should be sought primarily among the variables that modify the oyster population potential for recruitment, growth, and fecundity. Obvious choices for potential triggering mechanisms are variations in environmental conditions, such as food supply, turbidity level, current flow, salinity, and temperature. Other factors that influence the ability of the oyster population to grow such as competition for food (i.e., mussels), variations in recruitment and juvenile mortality, and the ability of the oyster to resist disease also potentially affect the occurrence of epizootics.

Frequently, the factor(s) that triggers an epizootic occurs well before the detection of the event (Gill 1928), and once initiated, epizootics can persist during what would be considered normal or optimal conditions. Furthermore, only a small change in conditions may be needed to trigger an epizootic because populations often exist in quasiequilibrium with the disease (Anderson 1991, Lenski and May 1994). Thus, the simulations that were designed to investigate epizootic triggering mechanisms used food, temper-

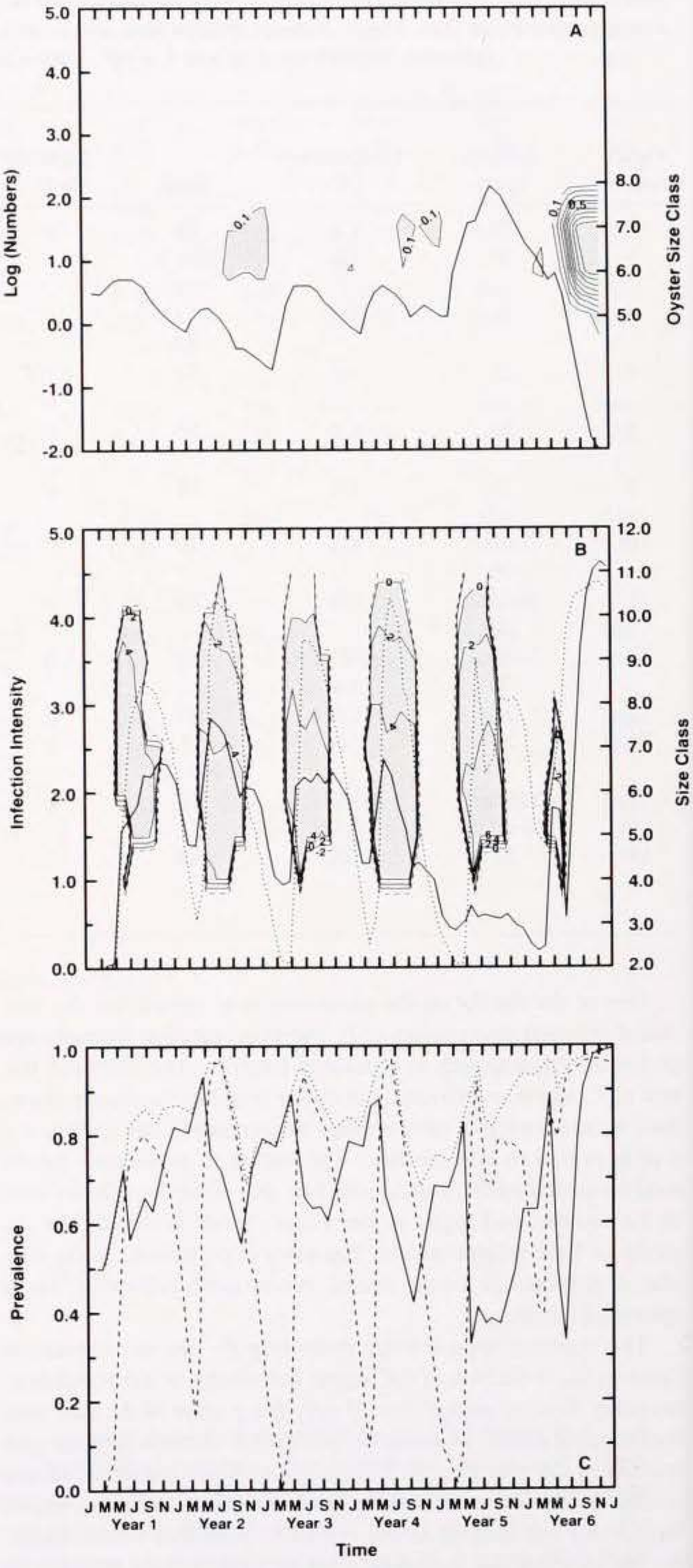

ature, salinity, and turbidity conditions for Galveston Bay in which 1 year of the 6-year time series was modified to introduce a small change in conditions. For each simulation, year 1 represented normal environmental conditions (as used for the simulation shown in Fig. 4), year 2 included the modified condition, and years 3 to 6 returned to normal conditions. Thus, the oyster populations were exposed to 5 years of environmental conditions that are conducive to growth and expansion (Fig. 4) and 1 year that potentially was not.

Food Supply

Decreased food supply reduces oyster growth and fecundity (Soniat and Ray 1985, Robinson 1992) but does not affect the cell division rate of *P. marinus*. Low food supply, then, is potentially an epizootic-triggering mechanism. However, the time during which oysters experience low food supply can be important because the rate of *P. marinus* division is temperature dependent. Thus, the effect of low food supply might be expected to be less in the winter than in the summer. In the following simulations, food supply in the second year was reduced by 0.25 mg l^{-1} for 4 months in either the winter or the summer, which gives a 10% decrease in food over the year.

A reduction in food supply during the winter has little impact on the oyster population (Fig. 5). Oyster ingestion rates are primarily a function of filtration rate which is temperature controlled. Decreased temperatures in the winter result in reduced filtration rates so that the impact of low food supply during this time is minimal. Moreover, the division rate of *P. marinus* is at its yearly low. Thus, low winter food supplies do not substantially alter the pattern of *P. marinus* prevalence and infection intensity from that seen in the reference simulation. *P. marinus* mortality is increased somewhat, but the oyster population continues to grow and expand.

By contrast, a reduction in food supply during the summer triggers an epizootic (Fig. 6). This epizootic contains all of the basic characteristics of most epizootics (e.g., Gill 1928, Plowright 1982, Shields and Kuris 1988). Although the reduced food supply occurs in the summer of the second year, the response of the oyster population is not immediately obvious and no dramatic mortality event occurs in the following year (year 3, Fig. 6A). In the next 2 years (4 and 5), however, the population declines to extinction as the primary phase of mortality begins 18 months after the triggering event (Fig. 6A).

Spawning continues during the entire epizootic phase and rates do not decline substantially until significant mortality begins in the adult population in year 5 (Fig. 6B). Fecundity through year 5 would be adequate for population recovery were *P. marinus* infection intensity to decline. Infection intensity rises persistently from about 3 in the summer and 1.5 in the winter of year 2 to above 4 in the summer and 2 in the winter in year 6 (Fig. 6B). The rise in infection intensity is most noticeable in the entire population rather than in the normally sampled market-size component because mortality in the latter size classes continually removes the most heavily infected individuals from the population.

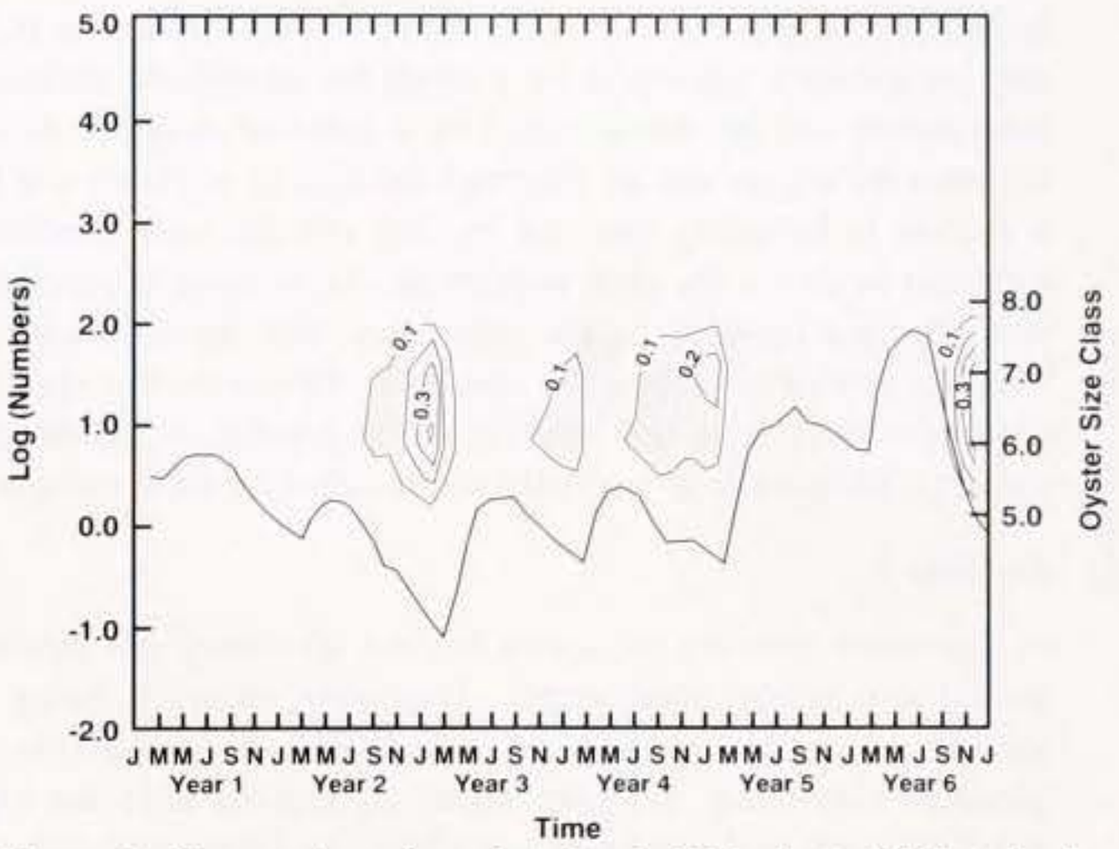

Figure 5. The number of market-size individuals (solid line) in the population expressed as $\log_{10}$(number m^{-2}), from a simulation that used environmental conditions that are characteristic of a high-salinity reef in Galveston Bay, TX (Table 5), that experienced a decline in food supply during the winter of year 2 (Table 6). Mortality events, calculated as the fraction of the population in a given size class that dies during a 1-month period, are indicated by the shaded contours, with an interval of 0.1.

During the epizootic, disease prevalence in the population gradually increases from about 60 to 80% to near 100% (Fig. 6C). However, prevalence, as usually measured (dotted line in Fig. 6C), changes little during the epizootic. Thus, false-negatives and inadequate sampling of the entire oyster size-frequency distribution can inhibit observation of this phase of disease intensification.

In this simulation, the population crash is not produced by a dramatic decrease in fecundity or recruitment. These are products of the crash. The population crash occurs because the rate of *P. marinus* growth and transmission exceeded the rate of expansion of the oyster population by just a small amount in year 2. A reduction in food supply during the summer months produces a subtle change in the balance between oyster population expansion and disease intensification which permits the disease to nudge ahead and gradually exert control over the host population. The initial food conditions for this simulation, which are typical of Galveston Bay, TX, allow population expansion but are near the threshold that can trigger an epizootic. For higher food supplies, a 10% decrease would have had a lesser effect. Thus, this simulation shows that a small change in environmental conditions may be all that is needed to generate an epizootic once the population nears the carrying capacity of the environment, and once the epizootic is triggered, simply returning to pretrigger environmental conditions

Figure 4. (A) The number of market-size individuals (solid line) in the population expressed as $\log_{10}$(number m^{-2}), from a simulation that used environmental conditions that are characteristic of a high-salinity reef in Galveston Bay, TX (Table 5). Mortality events, calculated as the fraction of the population in a given size class that dies during a 1-month period, are indicated by the shaded contours, with an interval of 0.1. (B) Simulated oyster population reproductive effort (shading) expressed as $\log_{10}$(total joules spawned per month) in each size class. Contour interval is 2 log units. *P. marinus* infection intensity expressed in terms of Mackin's (1962) 0- to 5-point scale is shown for the entire population (solid line) and the market-size (≥3-inch) portion of the population (dotted line). (C) *P. marinus* prevalence expressed as the fraction of the total population that is infected. Prevalences in the entire oyster population, the market-size (≥3-inch) portion of the oyster population, and the market-size population, assuming that all infections ≤2^{12} cells ind^{-1} are judged negative using the method described by Ray (1966), are represented by the solid, dotted, and dashed lines, respectively.

is insufficient to prevent disaster. Moreover, the simulation shows that an epizootic generated by a small but significant decline in food supply can be characterized by a delay of about 18 months between the trigger and an observed increase in mortality and that a decline in fecundity may not become obvious until significant mortality begins in the adult population. An increase in prevalence and infection intensity in the population may serve as an early warning sign of an impending epizootic. However, this rise may only be noticeable in that fraction of the population smaller than market size, a fraction normally not sampled by field surveys.

Turbidity

Increased turbidity decreases feeding efficiency and therefore should also restrict food supply. Increasing turbidity during the summer of year 2 to 10 mg l^{-1} (Table 5) initiates an epizootic that produces significant mortality about 12 months after the high-turbidity event and results in a crash of the oyster population in year 4 (Fig. 7). The simulated disease prevalence and intensity associated with this event are essentially identical to those obtained for the reduced food scenario (Fig. 6).

Current Flow

Certain combinations of food content, population density, and current flow may significantly affect the flux of food over the oyster reef (Muschenheim 1987, Wilson-Ormond et al. in press). A reduction in current flow during the four summer months of year 2 gives results that are similar to those shown for reduced food conditions. Significant oyster mortality begins about 18 months after the low-flow event and the population eventually crashes in years 5 and 6 (Fig. 8). The pattern of intensification of *P. marinus* infection in this and the reduced food simulation is similar, but the epizootic that results from low current flow develops more slowly.

Mussels

Competition from other filter feeders may reduce food supply and thus adversely impact the oyster population. In Texas bays, mussels of the genus *Brachidontes* are abundant. To provide a simulation comparable to the low-food, increased turbidity, and low-flow simulations, the mussels were allowed to impact food supply for only the summer months in year 2. The competing effect of the mussels acts to decrease the food supply to the oysters. The time-dependent evolution of the oyster population (Fig. 9) is similar to that shown in Figure 6 and the pattern of disease intensification and intensity is essentially identical to that seen in Figure 6B and C. An epizootic triggered in year 2 results in significant mortality about 18 months later and the population begins to decline in years 4 and 5 (Fig. 9).

Salinity

Small changes in climate have been shown to significantly modify recruitment to marine populations (Turrell et al. 1992) and disease (Jarosz and Burden 1992). *P. marinus* responds to temperature and salinity variations and even small perturbations in these environmental conditions arising from changes in climate can significantly modify *P. marinus* disease intensity over large geographic areas (Powell et al. 1992a). High-salinity conditions have a greater impact during the warmer half of the year. Temperature has a major effect in winter through its influence on parasite division rate and mortality.

The effect of salinity was investigated by raising salinity by 15

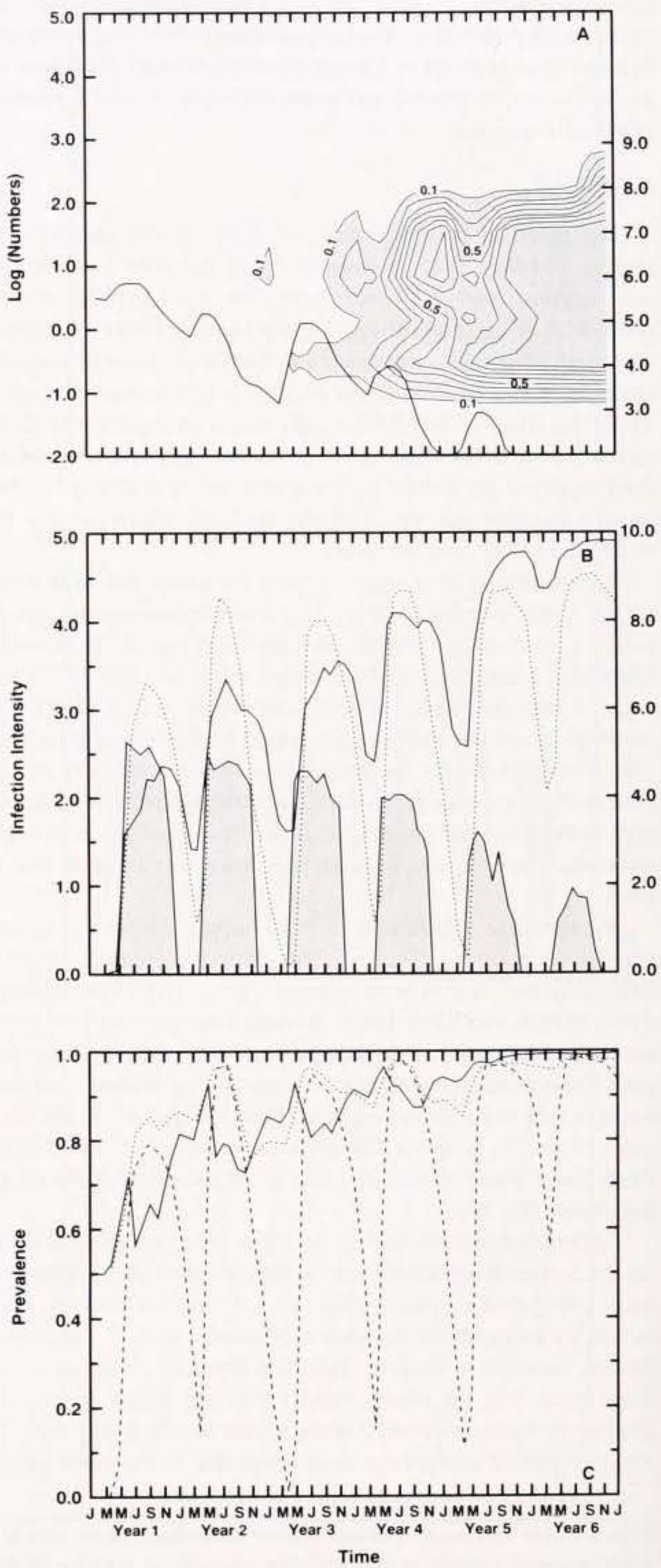

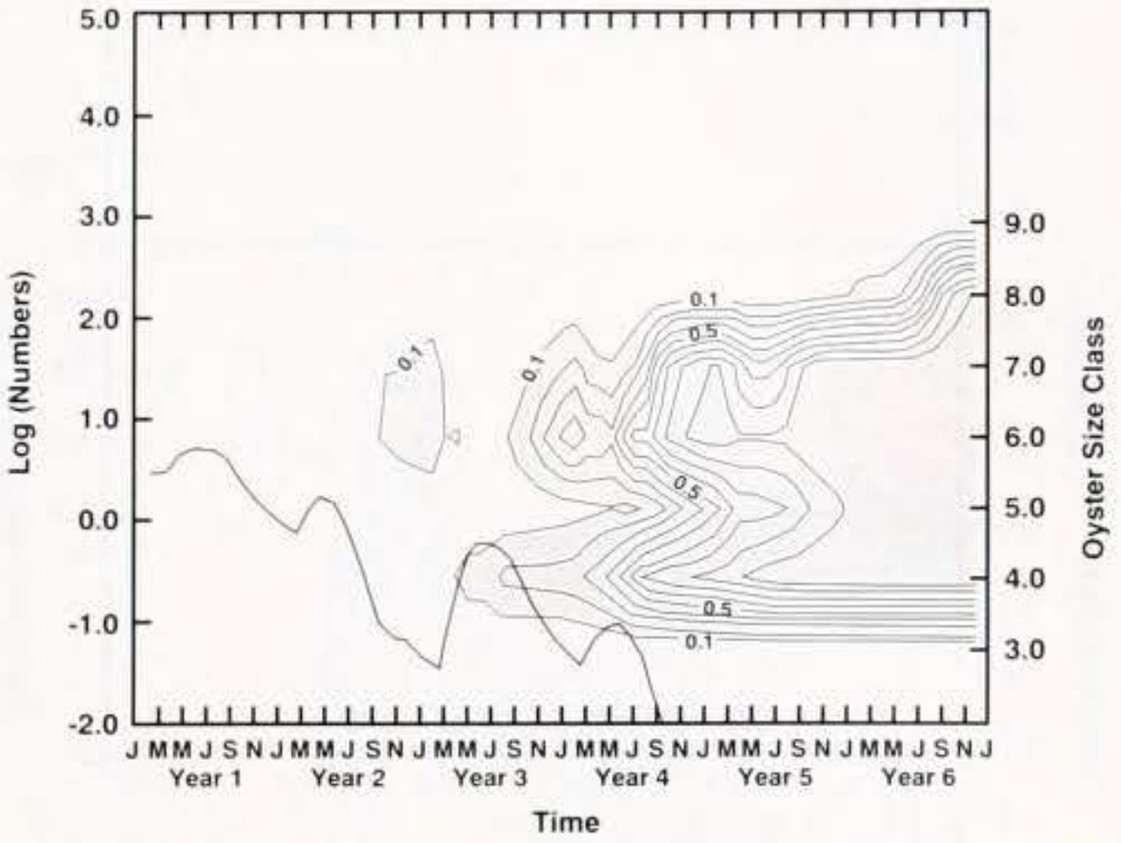

Figure 7. The number of market-size individuals (solid line) in the population expressed as $\log_{10}$(number m^{-2}), from a simulation that used environmental conditions that are characteristic of a high-salinity reef in Galveston Bay, TX (Table 5), that experienced an increase in turbidity during the summer of year 2 (Table 6). Mortality events, calculated as the fraction of the population in a given size class that dies during a 1-month period, are indicated by the shaded contours, with an interval of 0.1.

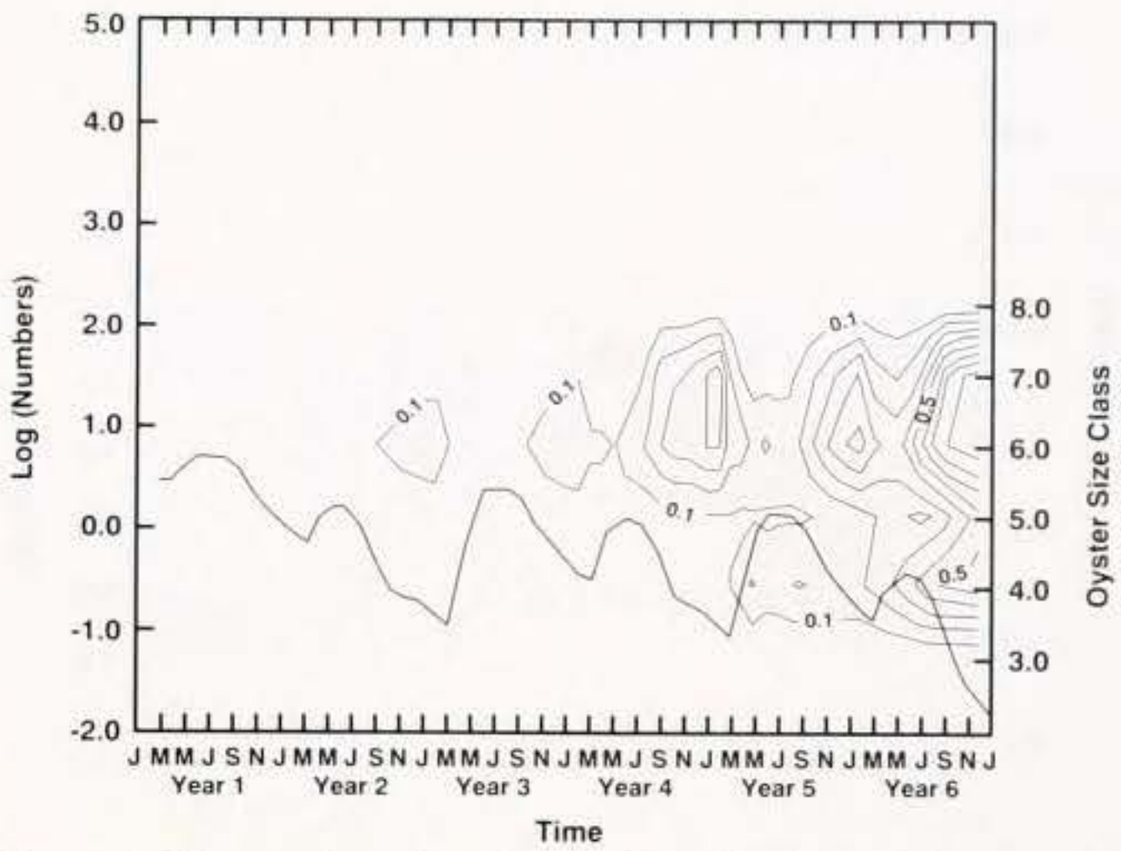

Figure 8. The number of market-size individuals (solid line) in the population expressed as $\log_{10}$(number m^{-2}), from a simulation that used environmental conditions that are characteristic of a high-salinity reef in Galveston Bay, TX (Table 5), that experienced a decrease in current flow during the summer of year 2 (Table 6). Mortality events, calculated as the fraction of the population in a given size class that dies during a 1-month period, are indicated by the shaded contours, with an interval of 0.1.

ppt for 6 months, April to September, in year 2. Increased salinity during the warmer months reduces the rate of population growth in comparison to the simulation that used normal conditions (cf. Fig. 4) by increasing the mortality of market-size oysters from *P. marinus*. However, an epizootic does not occur (Fig. 10). High-salinity is usually associated with epizootics (e.g., Crosby and Roberts 1990, Mann et al. 1991). However, many of the oyster populations in the Gulf of Mexico exist at salinities above 20 ppt for much or all of the year and maintain productive and expanding populations. High salinity may facilitate the development of an epizootic, but high salinity alone is unlikely to trigger one.

Exposing an oyster population to a 10-ppt decrease in salinity for 6 months, however, produces an immediate mortality event, which continues for an indefinite time (Fig. 11A). During the low-salinity event, infection intensity (Fig. 11B) and prevalence (Fig. 11C), as usually measured, decline as expected. However, the population prevalence and infection intensity rise as individuals of market-size decline, which is counterintuitive. Low salinity restricts scope for growth, and in the absence of a balancing effect such as increased food supply, this decrease restricts oyster growth, particularly in individuals already growth restricted by high *P. marinus* infection intensity (e.g., Menzel and Hopkins 1955). Such a growth restriction would be just enough, in heavily infected oysters, to produce a lethal infection. It is well known that oysters are more sensitive to low-salinity mortality during the summer months (e.g., Gunter 1953, Ray 1987, E. Powell unpublished data). This simulation suggests that *P. marinus* infection may be one important reason for this sensitivity, although no observations are available to support this speculation. Furthermore, the dramatic decrease in prevalence and infection intensity noted during and after low-salinity events in the summer (e.g., Soniat 1985) may well be due as much to the removal of heavily infected individuals from the population as to inhibition of *P. marinus* intensification. No evidence from field observations is available to support or refute this suggestion.

Temperature

Water temperature variation in Gulf of Mexico bays and estuaries between warm and cold years is rarely more than 2°C from the long-term mean (Sittel 1994). A change in temperature of this magnitude failed to initiate an epizootic. Frequently, however, extremely warm years co-occur with extremely dry years (about 10% of all years) in Galveston Bay and these years may be characterized by relatively warm winters or relatively warm summers. To test these effects, the summer temperature for the Galveston Bay time series was increased by 2°C (Table 5) and used with the summer salinity conditions that produced the simulated oyster population shown in Figure 10. The resultant extremely warm and dry summer produced a simulated oyster population distribution that was not significantly different from that shown in Figure 10. One reason is that summer conditions in the Gulf of Mexico are

Figure 6. (A) The number of market-size individuals (solid line) in the population expressed as $\log_{10}$(number m^{-2}), from a simulation that used environmental conditions that are characteristic of a high-salinity reef in Galveston Bay, TX (Table 5), that experienced a decline in food supply during the summer of year 2 (Table 6). Mortality events, calculated as the fraction of the population in a given size class that dies during a 1-month period, are indicated by the shaded contours, with an interval of 0.1. (B) Simulated oyster population reproductive effort (shading) expressed as $\log_{10}$(total calories spawned per month). *P. marinus* infection intensity expressed in terms of Mackin's (1962) 0- to 5-point scale is shown for the entire population (solid line) and the market-size (≥3-inch) portion of the population (dotted line). (C) *P. marinus* prevalence expressed as the fraction of the total population that is infected. Prevalences in the entire oyster population, the market-size (≥3-inch) portion of the oyster population, and the market-size population, assuming that all infections ≤2^{12} cells ind^{-1} are judged negative using the method described by Ray (1966), are represented by the solid, dotted, and dashed lines, respectively.

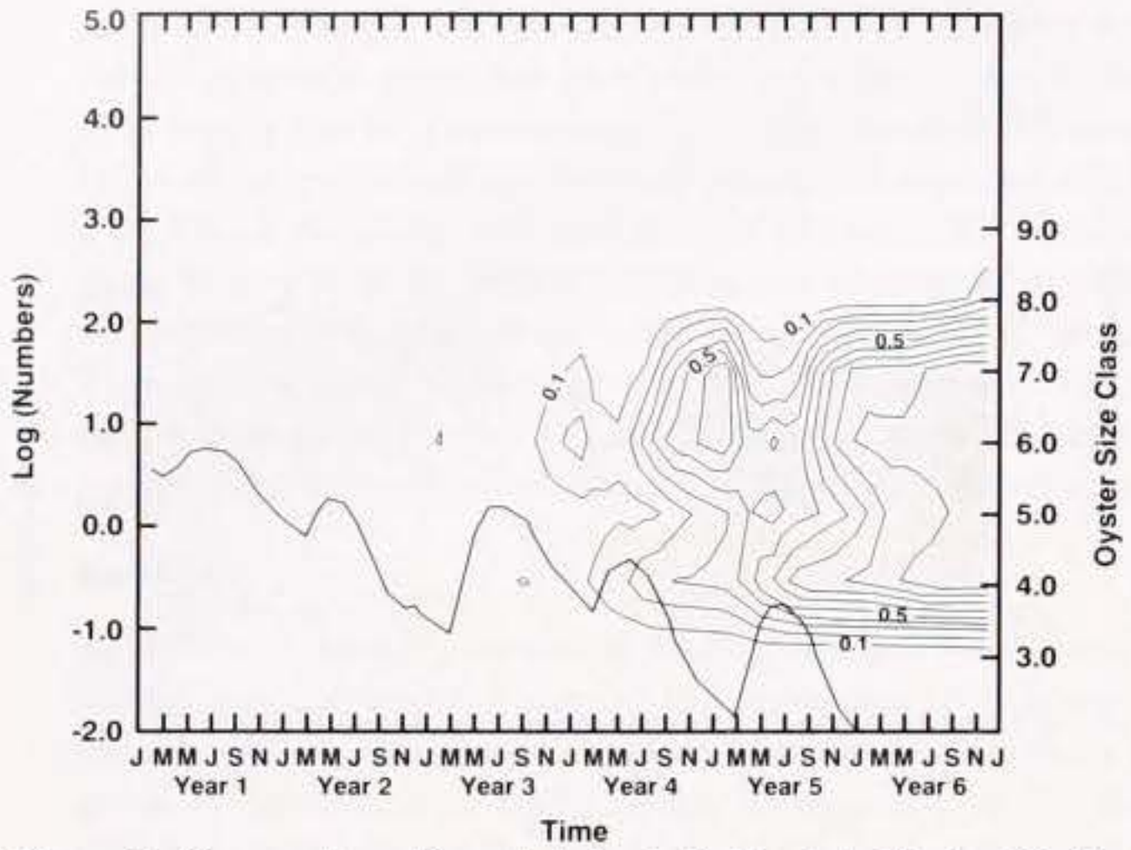

Figure 9. The number of market-size individuals (solid line) in the population expressed as $\log_{10}$(number m^{-2}), from a simulation that used environmental conditions that are characteristic of a high-salinity reef in Galveston Bay, TX (Table 5), that experienced a competitive interaction with mussels during Julian Days 450 to 630 (Table 6). Mortality events, calculated as the fraction of the population in a given size class that dies during a 1-month period, are indicated by the shaded contours, with an interval of 0.1.

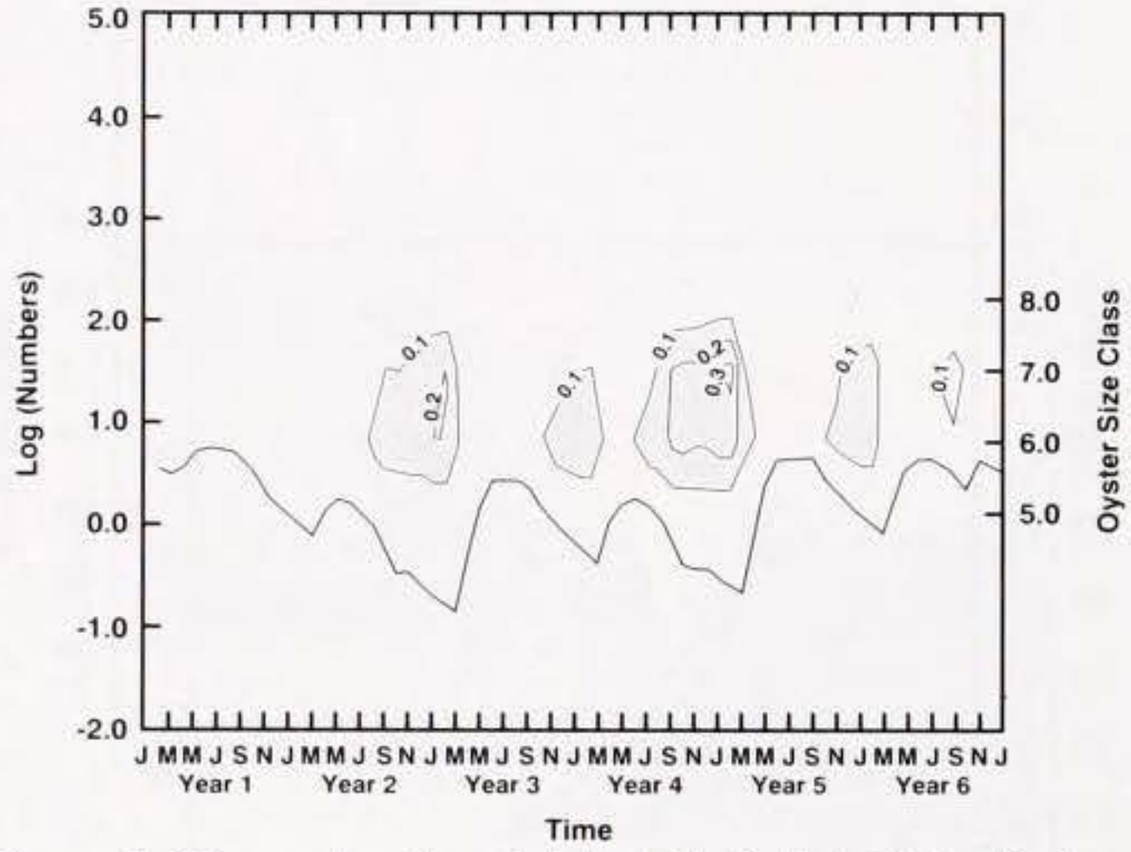

Figure 10. The number of market-size individuals (solid line) in the population expressed as $\log_{10}$(number m^{-2}), from a simulation that used environmental conditions that are characteristic of a high-salinity reef in Galveston Bay, TX (Table 5), that experienced a high-salinity event during the summer of year 2 (Table 6). Mortality events, calculated as the fraction of the population in a given size class that dies during a 1-month period, are indicated by the shaded contours, with an interval of 0.1.

already so conducive to *P. marinus* intensification that slightly warmer conditions have very little additional impact. Oyster populations must routinely withstand warm, dry summers to maintain the population abundances normally observed.

The same is not the case for a warmer winter. For this simulation, the winter water temperatures from Galveston Bay were increased by 2°C (Table 5) and used with the higher summer salinity conditions (Fig. 10) to produce a dry summer following a warm winter. These conditions produce a classic *P. marinus* epizootic (Fig. 12) which is similar in all respects to those described in previous simulations (e.g., Figs. 6–8). A warm winter increases the ratio of parasite division rate to parasite mortality rate so that winter infection intensities remain relatively high. This simulation suggests that the coincidences of appropriate summer salinities and winter temperatures are the environmental factors that contribute the most to the generation of an epizootic in Gulf of Mexico bays and estuaries.

Recruitment and Juvenile Mortality

Factors that affect population fecundity, recruitment, or juvenile mortality may destabilize host/parasite populations in quasiequilibrium (Dobson 1988). Decreasing recruitment success by 50% in the summer of year 2 (Julian days 450 to 630) or increasing juvenile mortality by 50% in the same time frame produced an epizootic qualitatively identical to the one depicted in Figure 6. The intensification of *P. marinus* infection closely followed the pattern shown in Figure 6B and C. An epizootic began to produce significant mortality about 12 months after the event, in each case, and the population crashed in years 4 and 5.

Changing Disease Resistance or Virulence

Resistance to disease is often important in initiating or stopping an epizootic (Ross 1982, Kent et al. 1989, McCallum 1990, Möller 1990). Although the development of resistance to *P. marinus* has been questioned (e.g., Lewis et al. 1992), Hofmann et al. (1995) suggested that some regional variation in oyster resistance or *P. marinus* virulence is probably required to explain regional variations in *P. marinus* prevalence and infection intensity. This effect was simulated by reducing the rate of parasite mortality $[r_m(T,S)]$ by changing the population halving time at 20°C–20 ppt from 60 to 120 hours. Note that a reduction in population doubling time (increased virulence) would yield similar results. The resultant simulated oyster population undergoes an epizootic with mass mortality starting in year 3 (Fig. 13). The reduction in parasite mortality (or increase in parasite division time) primarily affects the winter drop in infection intensity and produces conditions similar to those produced by a warm winter. Variations in the rate of parasite division or mortality have little effect in the summer when parasite density effects exert a major control on the growth rate of the *P. marinus* population.

MECHANISMS FOR STOPPING AN EPIZOOTIC

General Considerations

Once started, an epizootic is difficult to stop. In most cases, epizootics cease when the host population's density drops to a

Figure 11. (A) The number of market-size individuals (solid line) in the population expressed as $\log_{10}$(number m^{-2}), from a simulation that used environmental conditions that are characteristic of a high-salinity reef in Galveston Bay, TX (Table 5), that experienced a low-salinity event during the summer of year 2 (Table 6). Mortality events, calculated as the fraction of the population in a given size class that dies during a 1-month period, are indicated by the shaded contours, with an interval of 0.1. (B) *P. marinus* infection intensity expressed in terms of Mackin's (1962) 0- to 5-point scale is shown for the entire population (solid line) and the market-size (≥3-inch) portion of the population (dotted line). (C) *P. marinus* prevalence expressed as the fraction of the total population that is infected. Prevalences in the entire oyster population, the market-size (≥3-inch) portion of the oyster population, and the market-size population, assuming that all infections ≤2^{12} cells ind^{-1} are judged negative using the method described by Ray (1966), are represented by the solid, dotted, and dashed lines, respectively.

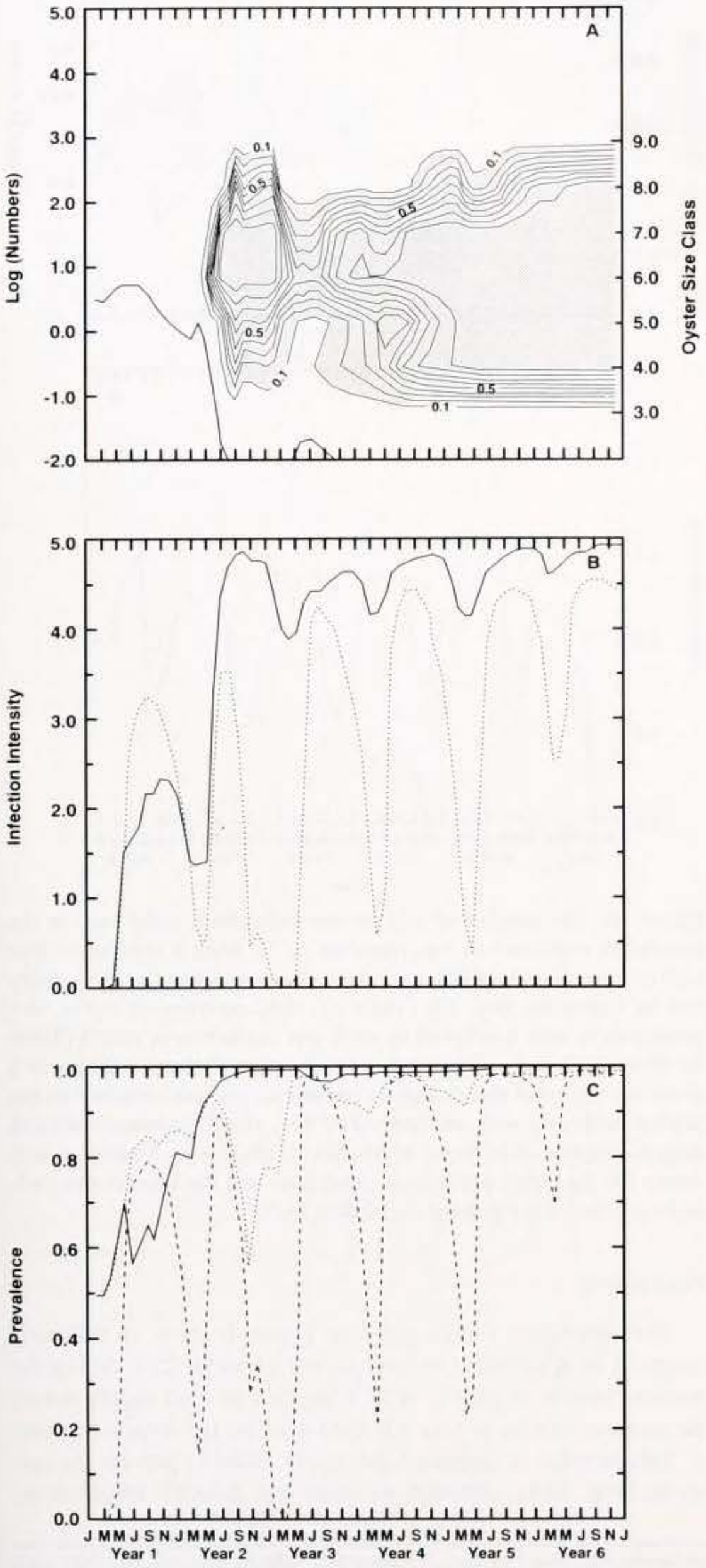

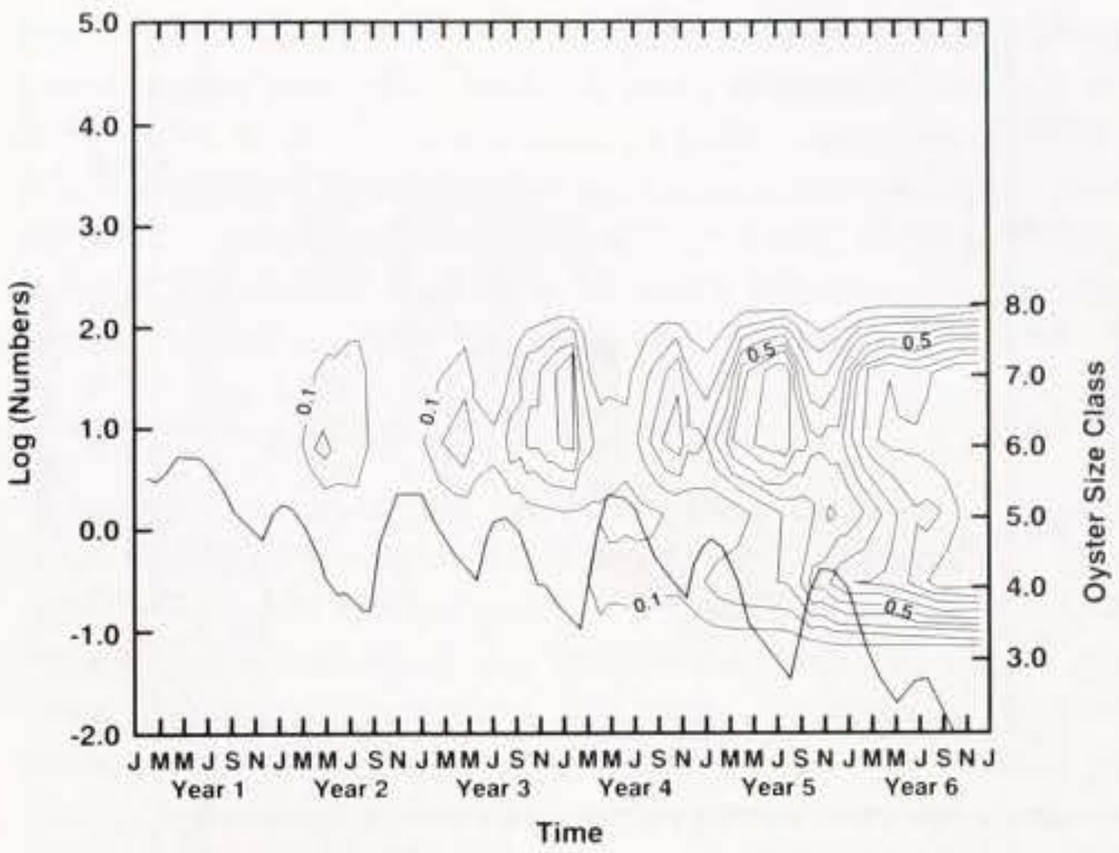

Figure 12. The number of market-size individuals (solid line) in the population expressed as $\log_{10}$(number m^{-2}), from a simulation that used environmental conditions that are characteristic of a high-salinity reef in Galveston Bay, TX (Table 5), that experienced a high-salinity event during the summer and a warm temperature event during the winter of year 2 (Table 6). Mortality events, calculated as the fraction of the population in a given size class that dies during a 1-month period, are indicated by the shaded contours, with an interval of 0.1.

critical level which is sufficiently low to inhibit transmission of the disease (Kermack and McKendrick 1991a,b, Anderson 1991). In most cases, this level is near local extinction, in comparison to densities normally found (e.g., Bartlett 1960, Plowright 1982, Ross 1982); this is especially true for *P. marinus* which has an efficient transmission mechanism even at low host densities. Thus, can epizootics be stopped by mechanisms other than local extinction?

Since triggering mechanisms normally are defined by small changes in some environmental or biological variable, small

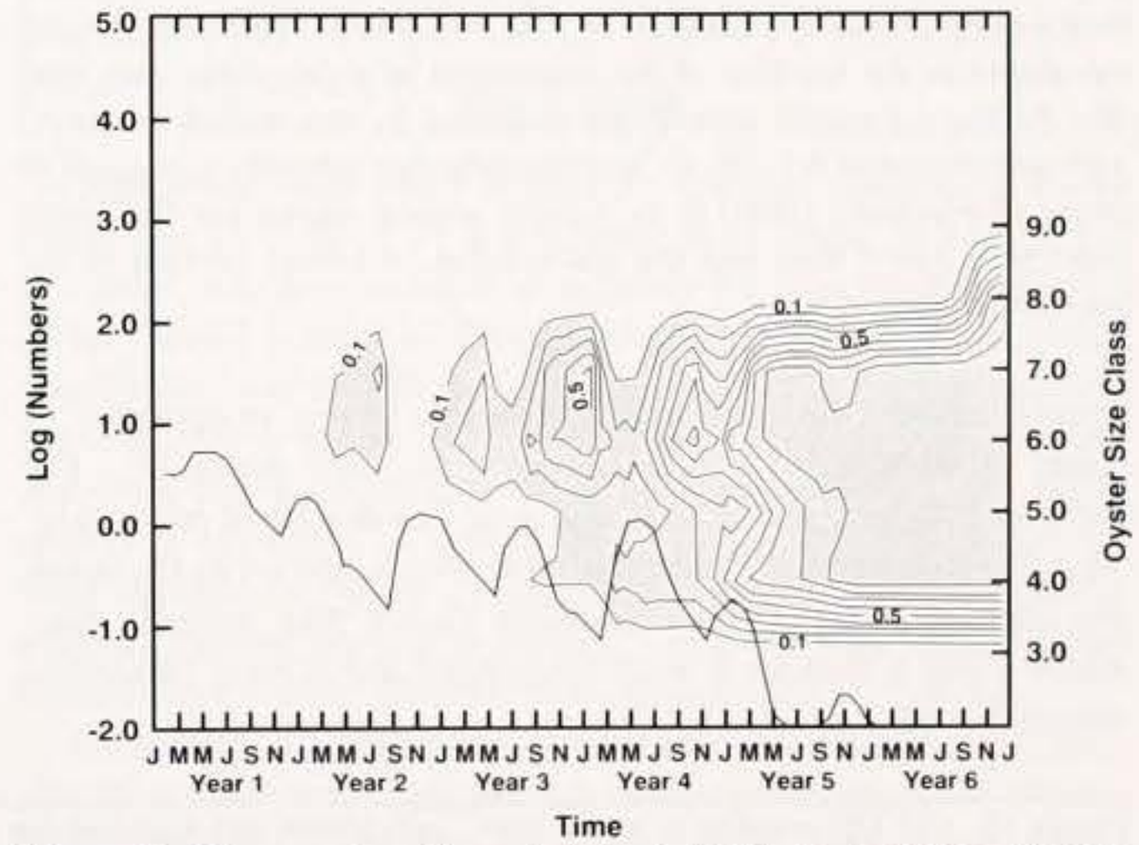

Figure 13. The number of market-size individuals (solid line) in the population expressed as $\log_{10}$(number m^{-2}), from a simulation that used environmental conditions that are characteristic of a high-salinity reef in Galveston Bay, TX (Table 5), that experienced a decrease in the rate of *P. marinus* cell mortality during the winter of year 2 (Table 6). Mortality events, calculated as the fraction of the population in a given size class that dies during a 1-month period, are indicated by the shaded contours, with an interval of 0.1.

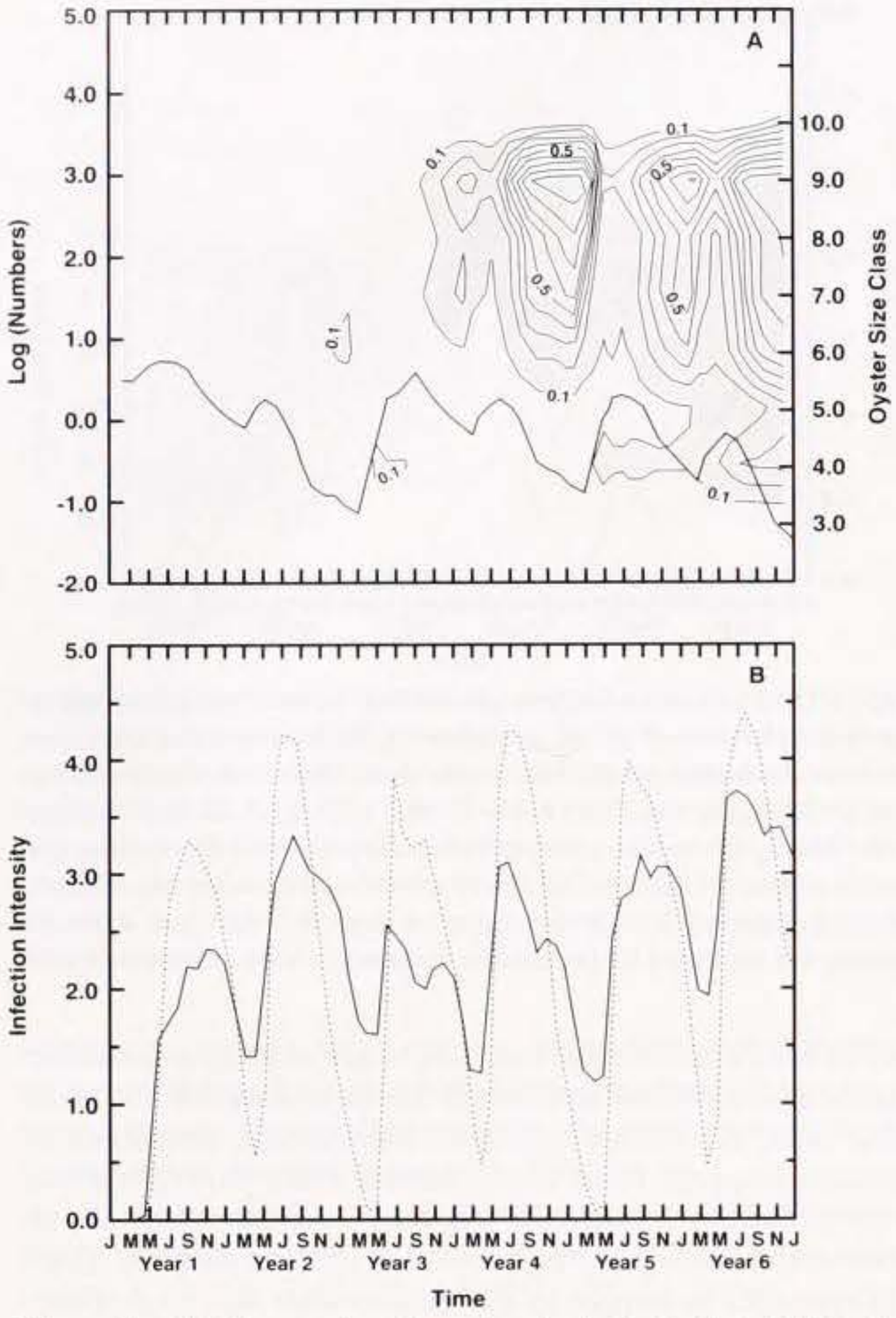

Figure 14. (A) The number of market-size individuals (solid line) in the population expressed as $\log_{10}$(number m^{-2}), from a simulation that used environmental conditions that are characteristic of a high-salinity reef in Galveston Bay, TX (Table 5), that experienced a decline in food supply during the summer of year 2 followed by an increase in food supply during the summer of year 3 (Table 6). Mortality events, calculated as the fraction of the population in a given size class that dies during a 1-month period, are indicated by the shaded contours, with an interval of 0.1. (B) *P. marinus* infection intensity expressed in terms of Mackin's (1962) 0- to 5-point scale is shown for the entire population (solid line) and the market-size (≥3-inch) portion of the population (dotted line).

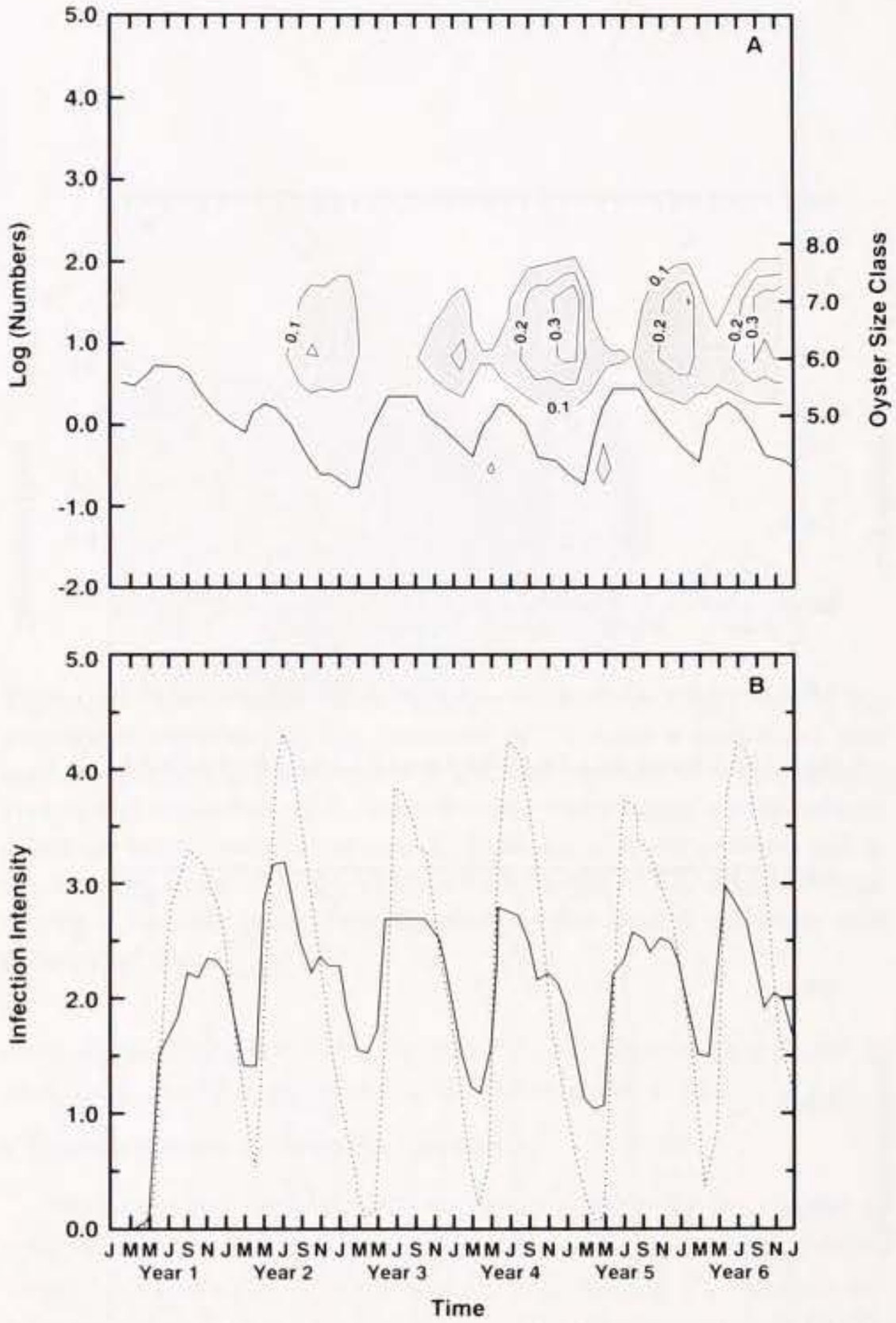

Figure 15. The number of market-size individuals (solid line) in the population expressed as $\log_{10}$(number m^{-2}), from a simulation that used environmental conditions that are characteristic of a high-salinity reef in Galveston Bay, TX (Table 5), that experienced warm, dry conditions in year 2 followed by cool, wet conditions in year 3 (Table 6). Mortality events, calculated as the fraction of the population in a given size class that dies during a 1-month period, are indicated by the shaded contours, with an interval of 0.1. (B) *P. marinus* infection intensity expressed in terms of Mackin's (1962) 0- to 5-point scale is shown for the entire population (solid line) and the market-size (≥3-inch) portion of the population (dotted line).

changes in these variables may also be able to stop an epizootic. A series of simulations was designed to test this possibility. For each, an epizootic was triggered in year 2 as described previously. Year 3 environmental conditions were then modified in the opposite direction to produce a favorable (better than normal) year. Years 1 and 4 through 6 were unchanged and normal conditions prevailed.

Food Supply

The simulation results given in Figure 6 show an epizootic triggered by a decrease in food supply of about 25% during the summer months of year 2. A 75% increase in food supply during the summer months of year 3 is used to offset the decrease in year 2. This increase in summer food supply failed to prevent the epizootic (Fig. 14A), although its onset was delayed. Infection in-

Figure 16. (A) The number of market-size individuals (solid line) in the population expressed as $\log_{10}$(number m^{-2}), from a simulation that used environmental conditions that are characteristic of a high-salinity reef in Galveston Bay, TX (Table 5), that experienced a decline in recruitment rate during the summer of year 2 followed by an increase in recruitment rate during the summer of year 3 (Table 6). Mortality events, calculated as the fraction of the population in a given size class that dies during a 1-month period, are indicated by the shaded contours, with an interval of 0.1. (B) *P. marinus* infection intensity expressed in terms of Mackin's (1962) 0- to 5-point scale is shown for the entire population (solid line) and the market-size (≥3-inch) portion of the population (dotted line). (C) *P. marinus* prevalence expressed as the fraction of the total population that is infected. Prevalences in the entire oyster population, the market-size (≥3-inch) portion of the oyster population, and the market-size population, assuming that all infections $\leq 2^{12}$ cells ind^{-1} are judged negative using the method described by Ray (1966), are represented by the solid, dotted, and dashed lines, respectively.

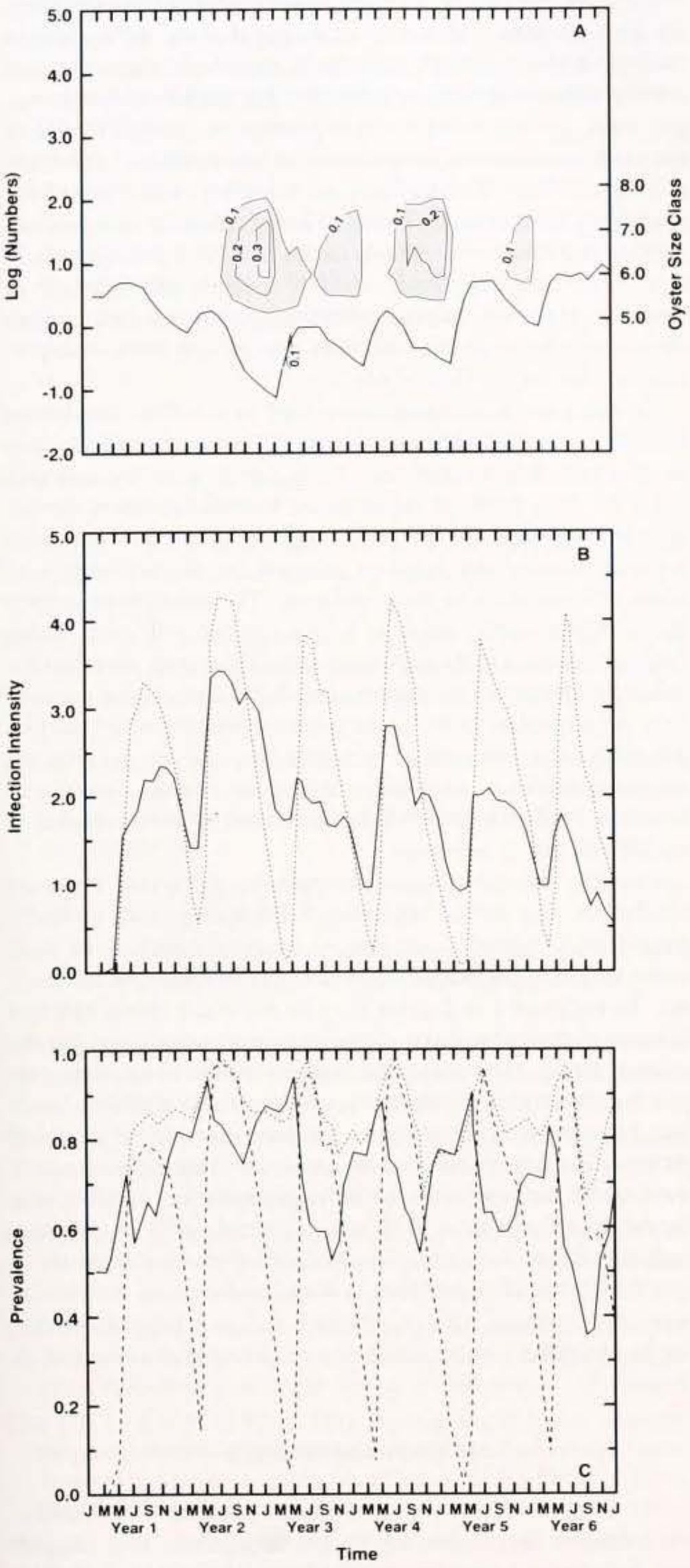

tensity is reduced in year 3 but then rises back to epizootic levels in subsequent years (Fig. 14B). A lesser increase of food (25 to 50%) failed to delay the epizootic, so that stopping an epizootic requires a much higher proportional increase in food supply than the decrease that triggered it. This occurs because of the inhibiting effect of high infection intensity on oyster filtration rate. Heavily infected oysters are food limited by their disease.

Temperature and Salinity

For the simulation shown in Figure 15, a warm dry year (year 2) was followed by a cool wet year in year 3. The cool wet year contained winter temperatures 2°C cooler than the standard Galveston Bay conditions and summer salinities that were 5 ppt fresher (Table 6). With these conditions, an epizootic fails to develop. Population abundances remain more or less stable, as does *P. marinus* mortality (Fig. 15A), prevalence, and infection intensity (Fig. 15B). Thus, a cool wet year following a warm dry year is sufficient to terminate an epizootic.

Recruitment and Juvenile Mortality

The decrease in recruitment in year 2 used for the simulation shown in Figure 6 was a 50% reduction from 2 in 10^9 to 1 in 10^9 between March and August. Offsetting this decrease required a recruitment success of 6 in 10^9 during the same period in year 3. The decrease in recruitment produces a mortality event, which is the beginning of an epizootic, in year 2 (Fig. 16A). The start of the epizootic is also identified by an increase in infection intensity (Fig. 16B) and prevalence (Fig. 16C). These trends are offset by increased recruitment success in year 3 as evidenced by decreases in prevalence and infection intensity that continue for the remaining 3 years of the simulation. As seen in other simulations, the primary record of the epizootic is found in the prevalence and infection intensity for the entire population rather than in the market-size individuals (Fig. 16B and C). Population abundance and mortality from *P. marinus* infection return to normal by year 4 and retain the characteristics of an expanding population (cf. Fig. 4) for the remainder of the simulation (Fig. 16A).

DISCUSSION

Thresholds exist which trigger *P. marinus* epizootics. These thresholds are defined by a combination of oyster fecundity, recruitment, and growth which determines the population dynamics of the species relative to the capabilities of its parasite. In oyster populations near the threshold, subtle changes in the environment are sufficient to trigger an epizootic. How frequently populations approach threshold conditions is unclear; however, the infrequency of epizootics in light of the small environmental perturbations required to trigger an epizootic in a susceptible population suggests that the population dynamics of most populations allows them to reside some distance from the epizootic threshold.

Epizootics are triggered by three general classes of environmental and biological perturbations: factors affecting food supply, factors affecting environmental characteristics, and factors affecting the supply of juveniles in the population. Factors affecting food supply include food supply itself, turbidity, competition with other filter-feeding species, and current flow. Environmental characteristics are principally temperature and salinity. Factors affecting the supply of juveniles include settlement success and juvenile mortality. Each of these interferes in one way or another with the rate at which populations recruit adult individuals.

In the common case where prevalence exceeds 60% and infection intensity rises to 3 or more during the summer months, most oyster populations will suffer adult mortality due to *P. marinus*. Stability is maintained by an adequate rate of adult replacement to minimize the effect of these losses on adult density and population fecundity. These recruits not only eventually maintain population fecundity, but also they replace heavily infected individuals with those with lighter infections. Epizootics are triggered when adult recruitment fails to replace those adults that die with adults of lower infection intensity at a rate adequate enough to dilute the adult infection intensity below about 3.5. The simulations show that one of the key changes in the population is the increase in infection intensity of the subadult and submarket-size adult portions of the population.

Accordingly, the simulations suggest that the key to triggering an epizootic is to raise the infection intensity in the subadult and submarket-size adult portions of the population, and indeed, most of the triggering mechanisms do just that. Infection intensity of market-size individuals is maintained at a relatively stable level by the death of heavily infected individuals. Consequently, an increase in the infection intensity of market-size individuals is normally neither obvious nor important. If the simulations are correct, it is ironic that the standard methods used to assess field infection intensities in *P. marinus* select for that fraction of the population least likely to provide information on the health of the population and least likely to provide early warning signals of an impending epizootic.

Ranking the triggering mechanisms by their ability to generate an epizootic is relatively difficult. Some of the variables, like temperature, do not vary over a wide range. Others, like recruitment, vary over orders of magnitude. The simulated conditions have been chosen to fit within the range of the variable as usually observed in the field. Based on these simulations, a rough ranking would suggest that factors affecting food supply are more likely to trigger epizootics than changes in temperature and salinity. The duration of the trigger is also important, however, and conditions conducive to the triggering of an epizootic may remain present longer for temperature and salinity than for food supply. One of the problems in assessing the importance of these variables in oyster populations is the limited information available on triggers of observed epizootics.

The characteristics of a developing epizootic were identical for all triggering mechanisms except low salinity. A drop in salinity resulted in an immediate mortality event suggestive of mortality due simply to low-salinity conditions as normally described for the warm months of the year. Such events may be intensified by disease rather than being due simply to the low salinity present.

Excepting this unusual case, all other epizootics followed a typical time course observed for epizootics of most other invertebrate and vertebrate species. The conditions triggering the epizootic occurred and disappeared well before, and as much as 18 months before, the initiation of mortality in the population. Unfortunately, identifying triggering mechanisms for observed epizootics is likely to be difficult unless, by serendipity, a long-term time series of data is available for the affected population. Once started, most epizootics progressed more or less rapidly toward population extinction. No internal mechanism was available to limit their time course. In the intermediate period between the trigger and the first major mortality event, prevalence and infection intensity rose in the population; the majority of this rise was concentrated in the subadult and submarket-size adult fractions of the population.

One of the interesting outcomes of this set of simulations was the difficulty in generating an epizootic simply with changes in temperature and salinity. Temperature and salinity share the blame for most epizootics. However, many populations, particularly in the Gulf of Mexico, exist under conditions of high temperature and salinity without initiating an epizootic. Although evidence is meager, most epizootics may occur in populations stressed by one of the other mechanisms prior to the high-temperature and high-salinity conditions that facilitate the mortality event. One of the most likely is recruitment failure. Timely failure to introduce uninfected individuals into the population is likely a principal mechanism increasing population infection intensity and initiating an epizootic. However, in cases where temperature and salinity are the cause, it is the winter conditions that seem to be most important, at least for the Gulf of Mexico.

Stopping an epizootic may be hard to do. The simulations generally required conditions substantially more extreme to stop an epizootic than to start one. Accordingly, local extinction is likely the most common outcome and the most common mechanism of terminating the epizootic. Stopping an epizootic otherwise requires reducing the infection intensity in the submarket-size adults and subadults in the population. The simulations suggest that a principal mechanism is a large recruitment event which dilutes *P. marinus* in the population, although it does not affect the infection intensity of the market-size adults. One crucial message from these simulations is that the infection intensity of the market-size adults does not need to be reduced to stop an epizootic nor does it need to be raised to start one. It is the infection intensity of juveniles recruited to the adult population and of adults recruited to market size that is important.

Overall, the most important message from this series of simulations may be the implications for management of oyster populations. Clearly, apparently healthy populations may reside very near the threshold for an epizootic. Also, an epizootic may be triggered 1 to 2 years prior to the major mortality event defining it, depending upon the environmental conditions and the external supply of recruits to the population. The simulations suggest that identifying populations nearing epizootic mortality levels may be as easy as obtaining an adequate time course record of prevalence and infection intensity across the entire size-frequency spectrum of the population. Identifying populations residing near the epizootic threshold is likely to be extremely difficult. Whether such populations have specific population dynamics attributes or specific disease characteristics is not clear based on the simulations presented here. One possibility is that such populations cannot be identified without simulation modeling of the host and its disease.

ACKNOWLEDGMENTS

We thank Elizabeth Wilson-Ormond, Margaret Dekshenieks, and Stephanie Boyles for help in data acquisition. This research was supported by contract DACW64-91-C-0040 from the U.S. Army Corps of Engineers, Galveston District Office, and computer funds from the College of Geosciences and Maritime Studies Research Development Fund. Additional computer resources and facilities were provided through the Center for Coastal Physical Oceanography at Old Dominion University.

LITERATURE CITED

Ackerman, E., L. R. Elveback & J. P. Fox. 1984. *Simulation of Infectious Disease Epidemics*. Charles C. Thomas, Springfield, Illinois, 202 pp.

Anderson, R. M. 1991. Discussion: the Kermack-McKendrick epidemic threshold theorem. *Bull. Math. Biol.* 53:3–32.

Anderson, R. S., K. T. Paynter & E. M. Burreson. 1992. Increased reactive oxygen intermediate production by hemocytes withdrawn from *Crassostrea virginica* infected with *Perkinsus marinus*. *Biol. Bull.* 183:476–481.

Andrews, J. D. 1965. Infection experiments in nature with *Dermocystidium marinum* in Chesapeake Bay. *Chesapeake Sci.* 6:60–67.

Andrews, J. D. 1988. Epizootiology of the disease caused by the oyster pathogen *Perkinsus marinus* and its effects on the oyster industry. *Amer. Fish. Soc. Spec. Publ.* 18:47–63.

Andrews, J. D. & S. M. Ray. 1988. Management strategies to control the disease caused by *Perkinsus marinus*. *Amer. Fish. Soc. Spec. Publ.* 18:257–264.

Bartlett, M. S. 1960. The critical community size for measles in the United States. *J. Royal Stat. Soc. Ser. A* 123:37–44.

Baughman, J. L. & B. B. Baker, Jr. 1949. Oysters in Texas. *Texas Game Fish. Oyster Comm. Bull. 29, Mar. Lab. Ser. 1*, 38 pp.

Black, F. L. 1966. Measles endemicity in insular populations: critical community size and its evolutionary implication. *J. Theo. Biol.* 11: 207–211.

Brousseau, D. J., J. A. Baglivo & G. E. Lang, Jr. 1982. Estimation of equilibrium settlement rates for benthic marine invertebrates: its application to *Mya arenaria* (Mollusca: Pelecypoda). *U.S. Fish Wild. Ser. Fish. Bull.* 80:642–644.

Burrell, V. G., Jr., M. Y. Bobo & J. J. Manzi. 1984. A comparison of seasonal incidence and intensity of *Perkinsus marinus* between subtidal and intertidal oyster populations in South Carolina. *J. World Maricult. Soc.* 153:301–309.

Chanley, P. E. 1957. Survival of some juvenile bivalves in water of low salinity. *Proc. Natl. Shellfish. Assoc.* 48:52–65.

Cheng, T. C. 1983. Triggering of immunologic defense mechanisms of molluscan shellfish by biotic and abiotic challenge and its applications. *J. Mar. Tech. Soc.* 17:18–25.

Chintala, M. M. & W. S. Fisher. 1991. Disease incidence and potential mechanisms of defense for MSX-resistant and -susceptible Eastern oysters held in Chesapeake Bay. *J. Shellfish Res.* 10:439–443.

Choi, K.-S., E. N. Powell, D. H. Lewis & S. M. Ray. 1994. Instantaneous reproductive effort in female American oysters, *Crassostrea virginica*, measured by a new immunoprecipitation assay. *Biol. Bull.* 186:41–61.

Choi, K.-S., E. A. Wilson, D. H. Lewis, E. N. Powell & S. M. Ray. 1989. The energetic cost of *Perkinsus marinus* parasitism in oysters: quantification of the thioglycollate method. *J. Shellfish Res.* 8:125–131.

Chu, F-L. E. & K. H. Greene. 1989. Effect of temperature and salinity on in vitro culture of the oyster pathogen *Perkinsus marinus* (Apicomplexa: Perkinsea). *J. Invertebr. Pathol.* 53:260–268.

Chu, F-L. E. & J. F. La Peyre. 1993. Development of disease caused by the parasite *Perkinsus marinus* and defense-related hemolymph factors in three populations of oysters from Chesapeake Bay, USA. *J. Shellfish Res.* 12:21–27.

Craig, A., E. N. Powell, R. R. Fay & J. M. Brooks. 1989. Distribution of *Perkinsus marinus* in Gulf coast oyster populations. *Estuaries* 12:82–91.

Crosby, M. P. & C. F. Roberts. 1990. Seasonal infection intensity cycle of the parasite *Perkinsus marinus* (and an absence of *Haplosporidium* spp.) in oysters from a South Carolina salt marsh. *Dis. Aquat. Org.* 9:149–155.

Cummins, H., E. N. Powell, R. J. Stanton, Jr. & G. Staff. 1986. The size-frequency distribution in palaeoecology: the effects of taphonomic processes during formation of death assemblages in Texas bays. *Palaeontology (London)* 29:495–518.

Dame, R. F. 1976. Energy flow in an intertidal oyster population. *Estuarine Coastal Mar. Sci.* 4:243–253.

Dekshenieks, M. M., E. E. Hofmann & E. N. Powell. 1993. Environmental effects on the growth and development of *Crassostrea virginica* (Gmelin) larvae: a modeling study. *J. Shellfish Res.* 12:241–254.

Dobson, A. P. 1988. The population biology of parasite-induced changes in host behavior. *Quart. Rev. Biol.* 63:139–165.

Doering, P. H. & C. A. Oviatt. 1986. Application of filtration rate models to field populations of bivalves: an assessment using experimental mesocosms. *Mar. Ecol. Prog. Ser.* 31:265–275.

Dungan, C. F. & B. S. Roberson. 1993. Binding specificities of monoand polyclonal antibodies to the protozoan oyster pathogen *Perkinsus marinus*. *Dis. Aquat. Org.* 15:9–22.

Dwyer, G. & J. S. Elkinton. 1993. Using simple models to predict virus epizootics in gypsy moth populations. *J. Anim. Ecol.* 62:1–11.

Fenchel, T. & B. J. Finlay. 1983. Respiration rates in heterotrophic, free-living protozoa. *Microb. Ecol.* 9:99–122.

Fisher, W. S. 1988. *In vitro* binding of parasites (*Bonamia ostreae*) and latex particle by hemocytes of susceptible and insusceptible oysters. *Dev. Comp. Immunol.* 12:43–53.

Fisher, W. S., M. M. Chintala & M. A. Moline. 1989. Annual variation of estuarine and oceanic oyster *Crassostrea virginica* Gmelin hemocyte capacity. *J. Exp. Mar. Biol. Ecol.* 127:105–120.

Fisher, W. S., J. D. Gauthier & J. T. Winstead. 1992. Infection intensity of *Perkinsus marinus* disease in *Crassostrea virginica* (Gmelin, 1791) from the Gulf of Mexico maintained under different laboratory conditions. *J. Shellfish Res.* 11:363–369.

Fisher, W. S. & R. I. E. Newell. 1986. Salinity effects on the activity of granular hemocytes of American oysters, *Crassostrea virginica*. *Biol. Bull.* 170:122–134.

Fisher, W. S. & M. Tamplin. 1988. Environmental influence on activities and foreign-particle binding by hemocytes of American oysters, *Crassostrea virginica*. *Can. J. Fish. Aquat. Sci.* 45:1309–1315.

Ford, S. E. 1986. Comparison of hemolymph proteins from resistant and susceptible oysters, *Crassostrea virginicia*, exposed to the parasite *Haplosporidium nelsoni* (MSX). *J. Invertebr. Pathol.* 47:283–294.

Ford, S. E. 1992. Avoiding the transmission of disease in commercial culture of molluscs, with special reference to *Perkinsus marinus* (Dermo) and *Haplosporidium nelsoni* (MSX). *J. Shellfish Res.* 11: 539–546.

Ford, S. E. & H. H. Haskin. 1988. Comparison of in vitro salinity tolerance of the oyster parasite, *Haplosporidium nelsoni* (MSX) and hemocytes from the host, *Crassostrea virginica*. *Comp. Biochem. Physiol.* 90:183–187.

Gee, J. M. & J. T. Davey. 1986. Experimental studies on the infestation of *Mytilus edulis* (L.) by *Mytilicola intestinalis* Steuer (Copepoda, Cyclopoida). *J. Cons. Int. Explor. Mer* 42:254–264.

Gill, C. A. 1928. *The Genesis of Epidemics and the Natural History of Disease*. William Wood and Company, New York, 550 pp.

Goggin, C. L., K. B. Sewell & R. J. G. Lester. 1990. Tolerances of *Perkinsus* spp. (Protozoa, Apicomplexa) to temperature, chlorine and salinity. *J. Shellfish Res.* 9:145–148.

Gunter, G. 1953. The relationship of the Bonnet Carre Spillway to oyster beds in Mississippi Sound and the "Louisiana marsh," with a report on the 1950 opening. *Publ. Inst. Mar. Sci. Univ. Texas* 3:17–71.

Hadeler, K. P. & H. I. Freedman. 1989. Predator-prey populations with parasitic infection. *J. Math. Biol.* 27:609–631.

Hall, R. P. 1967. Nutrition and growth of protozoa. *In:* T-T. Chen (ed.). *Research in Protozoology*, vol. 1. Pergamon Press, New York, pp. 337–404.

Hibbert, C. J. 1977. Growth and survivorship in a tidal-flat population of bivalve *Mercenaria mercenaria* from Southampton Water. *Mar. Biol.* 44:71–76.

Hofmann, E. E., E. N. Powell, J. M. Klinck & G. Saunders. 1995. Mod-

eling diseased oyster populations. 1. Modeling *Perkinsus marinus* infections in oysters. *J. Shellfish Res.* 14:121–151.

Hofmann, E. E., E. N. Powell, J. M. Klinck & E. A. Wilson. 1992. Modeling oyster populations. III. Critical feeding periods, growth and reproduction. *J. Shellfish Res.* 11:399–416.

Hofstetter, R. P. 1977. Trends in population levels of the American oyster, *Crassostrea virginica* (Gmelin), on public reefs in Galveston Bay, Texas. *Texas Parks Wildl. Dept. Tech. Ser.* 24:1–90.

Hofstetter, R. P. 1990. The Texas oyster fishery. *Texas Parks Wildl. Dept. Bull.* No. 40, 21 pp.

Hunter, M. D. & P. W. Price. 1992. Playing chutes and ladders: heterogeneity and the relative roles of bottom-up and top-down forces in natural communities. *Ecology* 73:724–732.

Jakobsen, P. J., G. H. Johnsen & P. Larsson. 1988. Effects of predation risk and parasitism on the feeding ecology, habitat use, and abundance of lacustrine three spine stickleback (*Gasterosteus aculeatus*). *Can. J. Fish. Aquat. Sci.* 45:426–431.

Jarosz, A. M. & J. J. Burdon. 1992. Host-pathogen interactions in natural populations of *Linum marginale* and *Melampsora lini* III. Influence of pathogen epidemics on host survivorship and flower production. *Oecologia* 89:53–61.

Kent, M. L., R. A. Elston, M. T. Wilkinson & A. S. Drum. 1989. Impaired defense mechanisms in bay mussels, *Mytilus edulis*, with heroic neoplasia. *J. Invertebr. Pathol.* 53:378–386.

Kermack, W. O. & A. G. McKendrick. 1991a. Contributions to the mathematical theory of epidemics-I. *Bull. Math. Biol.* 53:33–55.

Kermack, W. O. & A. G. McKendrick. 1991b. Contributions to the mathematical theory of epidemics-II. The problems of epidemicity. *Bull. Math. Biol.* 53:57–87.

Laybourn-Parry, J. 1987. Protozoa. *In:* T. J. Pandian & F. J. Vernberg (eds.). *Animal Energetics, Vol. 1. Protozoa through Insecta.* Academic Press, Inc., New York, pp. 1–25.

Lenski, R. E. & R. M. May. 1994. The evolution of virulence in parasites and pathogens: reconciliation between two competing hypotheses. *J. Theor. Biol.* 169:253–265.

Lewis, E. J., F. G. Kern, A. Rosenfield, S. A. Stevens, R. L. Walker & P. B. Heffernan. 1992. Lethal parasites in oysters from coastal Georgia with discussion of disease and management implications. *Mar. Fish. Rev.* 54:1–6.

Lund, E. J. 1957. A quantitative study of clearance of a turbid medium and feeding by the oyster. *Publ. Inst. Mar. Sci. Univ. Texas* 4:296–312.

Mackin, J. G. 1952. Incidence of infection of oysters by *Dermocystidium* in the Barataria Bay area of Louisiana. *Natl. Shellfish Assoc. Conv. Add. for 1951*, 22–35.

Mackin, J. G. 1961. Mortality of oysters. *Proc. Natl. Shellfish. Assoc.* 50:21–40.

Mackin, J. G. 1962. Oyster disease caused by *Dermocystidium marinum* and other microorganisms in Louisiana. *Publ. Inst. Mar. Sci. Univ. Texas* 7:132–299.

Mackin, J. G. & J. L. Boswell. 1954. The relation of forced closure of oysters and acceleration of reproduction of *Dermocystidium marinum*. *Texas A&M Univ. Res. Found. Tech. Rep. Proj. 23* 17:1–6.

Mackin, J. G. & S. H. Hopkins. 1961. Studies on oyster mortality in relation to natural environments and to oil fields in Louisiana. *Publ. Inst. Mar. Sci. Univ. Texas* 7:1–131.

Mackin, J. G. & S. M. Ray. 1955. Studies on the effect of infection by *Dermocystidium marinum* on ciliary action in oysters (*Crassostrea virginica*). *Proc. Natl. Shellfish. Assoc.* 45:168–181.

Mann, R., E. M. Burreson & P. K. Baker. 1991. The decline of the Virginia oyster fishery in Chesapeake Bay: Considerations for introduction of a non-endemic species, *Crassostrea gigas* (Thunberg, 1793). *J. Shellfish Res.* 10:379–388.

May, E. B. 1971. A survey of the oyster and oyster shell resources of Alabama. *Ala. Mar. Res. Bull.* 4:1–53.

McCallum, H. I. 1990. Covariance in parasite burdens: the effect of predisposition to infection. *Parasitology* 100:153–159.

McCallum, H. I. & G. R. Singleton. 1989. Models to assess the potential of *Capillaria hepatica* to control population outbreaks of house mice. *Parasitology* 98:425–437.

Medcof, J. C. 1961. Oyster farming in the maritimes. *Bull. Fish. Res. Board Can.* 131:1–155.

Menzel, R. W. & S. H. Hopkins. 1955. The growth of oysters parasitized by the fungus *Dermocystidium marinum* and by the trematode *Bucephalus cuculus*. *J. Parasitol.* 41:333–342.

Möller, H. 1990. Association between diseases of flounder (*Platichthys flesus*) and environmental conditions in the Elbe estuary, FRG. *J. Cons. Int. Explor. Mer* 46:187–199.

Mollison, D. 1987. Population dynamics of mammalian diseases. *Symp. Zool. Soc. Lond.* 58:329–342.

Muschenheim, D. K. 1987. The dynamics of near-bed seston flux and suspension-feeding benthos. *J. Mar. Res.* 45:473–496.

Newell, R. I. E. 1985. Physiological effects of the MSX parasite *Haplosporidium nelsoni* (Haskin, Stauber & Mackin) on the American oyster *Crassostrea virginica* (Gmelin). *J. Shellfish Res.* 5:91–95.

NOAA. 1991. Recreational shellfishing in the United States. United States Department of Commerce, National Oceanic and Atmospheric Administration, 22 pp.

Ogle, J. & K. Flurry. 1980. Occurrence and seasonality of *Perkinsus marinus* (Protozoa: Apicomplexa) in Mississippi oysters. *Gulf Res. Rep.* 6:423–425.

Onstad, D. W. & J. V. Maddox. 1989. Modeling the effects of the microsporidium, *Nosema pyrausta*, on the population dynamics of the insect, *Ostrinia nubilalis*. *J. Invertebr. Pathol.* 53:410–421.

Paynter, K. T. & E. M. Burreson. 1991. Effects of *Perkinsus marinus* infection in the Eastern oyster, *Crassostrea virginica:* II. Disease development and impact on growth rate at different salinities. *J. Shellfish Res.* 10:425–431.

Plowright, W. 1982. The effects of rinderpest and rinderpest control on wildlife in Africa. *Symp. Zool. Soc. Lond.* 50:1–28.

Powell, E. N., H. Cummins, R. J. Stanton, Jr. & G. Staff. 1984. Estimation of the size of molluscan larval settlement using the death assemblage. *Estuarine Coastal Shelf Sci.* 18:367–384.

Powell, E. N., J. D. Gauthier, E. A. Wilson, A. Nelson, R. R. Fay & J. M. Brooks. 1992a. Oyster disease and climate change. Are yearly changes in *Perkinsus marinus* parasitism in oysters (*Crassostrea virginica*) controlled by climatic cycles in the Gulf of Mexico? P.S.Z.N.I.: *Mar. Ecol.* 13:243–270.

Powell, E. N., E. E. Hofmann, J. M. Klinck & S. M. Ray. 1992b. Modeling oyster populations I. A commentary on filtration rate. Is faster always better? *J. Shellfish Res.* 11:387–398.

Powell, E. N., E. E. Hofmann, J. M. Klinck, E. Wilson-Ormond & M. S. Ellis. 1995a. Modeling oyster populations V. Declining phytoplankton stocks and the population dynamics of American oyster (*Crassostrea virginica*) populations. *Fish. Res.* 24:199–222.

Powell, E. N., J. M. Klinck, E. E. Hofmann & S. M. Ray. 1994. Modeling oyster populations. IV. Population crashes and management. *U. S. Fish Wildl. Serv. Fish. Bull.* 92:347–373.

Powell, E. N., J. Song, M. S. Ellis & E. A.Wilson-Ormond. 1995b. The status and long-term trends of oyster reefs in Galveston Bay, Texas. *J. Shellfish Res.* 14:439–457.

Powell, E. N. & R. J. Stanton, Jr. 1985. Estimating biomass and energy flow of molluscs in paleo-communities. *Palaeontology* (*Lond*) 28:1–34.

Quick, J. A., Jr. & J. G. Mackin. 1971. Oyster parasitism by *Labyrinthomyxa marina* in Florida. *Fla. Dept. Nat. Res. Mar. Res. Lab. Prof. Paper Ser.* 13:1–55.

Ragone, L. M. & E. M. Burreson. 1993. Effect of salinity on infection progression and pathogenicity of *Perkinsus marinus* in the Eastern oyster, *Crassostrea virginicia* (Gmelin). *J. Shellfish Res.* 12:1–7.

Ray, S. M. 1954. Biological studies of *Dermocystidium marinum* a fungus parasite of oysters. *Rice Inst. Pamph. Monogr. Biol. Spec. Issue* 114 pp.

Ray, S. M. 1966. A review of the culture method for detecting *Dermo-*

cystidium marinum, with suggested modifications and precautions. *Proc. Natl. Shellfish. Assoc.* 54:55–69.

Ray, S. M. 1987. Salinity requirements of the American oyster, *Crassostrea virginicia*. *In:* A. J. Muller & G. A. Matthews (eds.). *Freshwater Inflow Needs of the Matagorda Bay System with Focus on the Needs of Penaeid Shrimp*. National Oceanic and Atmospheric Administration, Technical Memorandum NMFS-SEFC-189, pp. E.1–E.28.

Ray, S. M. & A. C. Chandler. 1955. *Dermocystidium marinum*, a parasite of oysters. *Exp. Parasitol.* 4:172–200.

Robinson, A. 1992. Dietary supplements for reproductive conditioning of *Crassostrea gigas kumamoto* (Thunberg). I. effects on gonadal development, quality of ova and larvae through metamorphosis. *J. Shellfish Res.* 11:437–441.

Ross, J. 1982. Myxomatosis: the natural evolution of the disease. *Symp. Zool. Soc. London* 50:77–95.

Saunders, G. L., E. N. Powell & D. H. Lewis. 1993. A determination of in vivo growth rates for *Perkinsus marinus*, a parasite of *Crassostrea virginica*. *J. Shellfish Res.* 12:229–240.

Schmid-Hempel, P. & R. Schmid-Hempel. 1988. Parasitic flies (Conopidae, Diptera) may be important stress factors for the ergonomics of their bumblebee hosts. *Ecol. Entomol.* 13:469–472.

Shields, J. D. & A. M. Kuris. 1988. Temporal variation in abundance of the egg predator *Carcinonemertes epialti* (Nemertea) and its effect on egg mortality of its host, the shore crab, *Hemigrapsus oregonensis*. *Hydrobiologia* 156:31–38.

Sindermann, C. J. 1993. Disease risks associated with importation of non-indigenous marine animals. *Mar. Fish. Rev.* 54:1–10.

Sittel, M. C. 1994. Marginal probabilities of the extremes of ENSO events for temperature and precipitation in the southeastern United States. Florida State University Technical Report, 94-1, 155 pp.

Soniat, T. M. 1985. Changes in levels of infection of oysters by *Perkinsus marinus*, with special reference to the interaction of temperature and salinity upon parasitism. *Northeast Gulf Sci.* 7:171–174.

Soniat, T. M. & M. S. Brody. 1988. Field validation of a habitat suitability index model for the American oyster. *Estuaries* 11:87–95.

Soniat, T. M. & S. M. Ray. 1985. Relationships between possible available food and the composition, condition and reproductive state of oysters from Galveston Bay, Texas. *Contrib. Mar. Sci.* 28:109–121.

Turrell, W. R. 1992. New hypotheses concerning the circulation of the northern North Sea and its relation to North Sea fish stock recruitment. *ICES J. Mar. Sci.* 49:107–123.

Warburton, F. E. 1958. Control of the boring sponge on oyster beds. *Fish. Res. Bd. Can. Prog. Rep. Atlantic Coast Stat.* 69:7–11.

Wells, H. W. 1961. The fauna of oyster beds, with special reference to the salinity factor. *Ecol. Monogr.* 31:239–266.

White, M. E., E. N. Powell & S. M. Ray. 1988. Effects of parasitism by the pyramidellid gastropod *Boonea impressa* on the net productivity of oysters (*Crassostrea virginica*). *Estuarine Coastal Shelf Sci.* 26:359–377.

Wilson, E. A., E. N. Powell, M. A. Craig, T. L. Wade & J. M. Brooks. 1990. The distribution of *Perkinsus marinus* in Gulf coast oysters: its relationship with temperature, reproduction, and pollutant body burden. *Int. Rev. Gesamten Hydrobiol.* 75:533–550.

Wilson-Ormond, E. A., E. N. Powell & S. M. Ray. in press. Short-term and small-scale variation in food availability to natural oyster populations: food, flow and flux. *P.S.Z.N.I.: Mar. Ecol.*

Wright, D. A. & E. W. Hetzel. 1985. Use of RNA:DNA ratios as an indicator of nutritional stress in the American oyster *Crassostrea virginica*. *Mar. Ecol. Progr. Ser.* 25:199–206.